



# Structural Design Sensitivity Analysis for Composites Undergoing Elastoplastic Deformation

A. CHATTOPADHYAY AND R. GUO

Department of Mechanical and Aerospace Engineering  
Arizona State University, Tempe, AZ 85287-6106, U.S.A.

(Received April 1994; accepted February 1995)

**Abstract**—Nonlinear structural design sensitivity analysis for structures undergoing elastoplastic deformation is developed in this paper. The reference volume concept is used to unify the shape and nonshape design problems. The rate (time-independent) constitutive model is employed to account for the plastic material behavior. In the response analysis, a higher order approximation procedure of the integration of the rate constitutive equations is proposed. The direct differentiation approach (DDA) is adopted to obtain the design sensitivity equation for the response variables. A method of partial differentiation of the rate constitutive equations, which yields a set of linear differential equations in the partial derivatives of stresses and internal variables with respect to the design variable, is included in the DDA procedure. In Part I of this paper, the general theory is described. In Part II, the theory is applied to a composite laminated beam problem.

**Keywords**—Composites, Direct differentiation, Design sensitivity, Elastoplasticity, Reference volume.

## NOMENCLATURE

${}^t b_i$	= body force per unit mass at load level $t$
$C_{ijkl}$	= linear elastic modulus
$d_i$	= design variable
${}^0 J, {}^0 J_\Gamma$	= Jacobian and area metric of the transformation ${}^0 x_i \rightarrow {}^r x_i$ , respectively
${}^t J, {}^t J_\Gamma$	= Jacobian and area metric of the transformation ${}^t x_i \rightarrow {}^0 x_i$ , respectively
${}^t Q_{ijkl}$	= elastoplastic stiffness
$T_i$	= ply thickness of the laminated beam
${}^t u_i$	= displacement field at load level $t$
${}^r x_i$	= coordinate in the fixed reference volume
${}^t x_i$	= coordinate at load level $t$
${}^t \varepsilon_{ij}$	= strain tensor at load level $t$
$\theta_i$	= ply angle of the laminated beam
${}^t \rho$	= mass per unit volume at load level $t$
${}^t \sigma_{ij}$	= Cauchy stress tensor at load level $t$
${}^t \varphi$	= curvature of the beam at load level $t$

The research was supported by the U.S. Army Research Office, Grant number DAAH04-93-G-0043. Technical monitor, G. Anderson.

Typeset by  $\mathcal{A}\mathcal{M}\mathcal{S}\text{-T}\mathcal{E}\mathcal{X}$

## INTRODUCTION

Design sensitivity, which means calculation of derivatives of the structural response quantities with respect to the design variables, has been a topic of interest to many researchers over the years. The sensitivity analysis for linear structural problems is a well studied area. Research has also been performed on nonlinear sensitivity analysis for isotropic materials. Three major techniques are commonly employed in the calculation of sensitivities. They are the finite difference technique, the direct differentiation approach and the adjoint variables approach. The simplest of course is the finite difference approach which is often computationally prohibitive. Tsay *et al.* [1] and Tsay *et al.* [2] presented the direct differentiation and the adjoint variable approaches for design sensitivity analysis (DSA) of nonlinear structural systems. Both geometric and material nonlinearities were included. The shape and nonshape design problems were unified using the reference volume concept. The design sensitivities at a particular load level were related to the design sensitivities at the previous load level. However, due to the discontinuities of the design sensitivities at the elastoplastic transition points, the sensitivities at the elastic level cannot be used in the calculation of the sensitivities at the following plastic level. Vidal *et al.* [3] have also discussed the design sensitivity analysis of history dependent problems. The constitutive model used in their study is continuously differentiable with respect to design parameters, so there is no discontinuity in the design sensitivities. Lee *et al.* [4] developed design sensitivity for elastoplastic structures. Discontinuities in the design sensitivities were investigated and procedures to treat them were discussed. A load incrementation procedure for the response analysis was presented which gives increments in the response variables. A direct variation approach was developed in which design variations of the equilibrium equations and the constitutive equations were used to calculate the design variations of the response variables. The method required integration of the variations of the constitutive equations. The design sensitivity expression was also discretized for numerical calculations using the isoparametric formulation of the finite element analysis.

The analytical investigation has primarily been in the area of isotropic materials. In the area of composites, the sensitivity of structures undergoing nonlinear deformation has not been addressed analytically. The purpose of the present paper is to discuss nonlinear design sensitivity analysis of anisotropic materials undergoing elastoplastic deformation. In Part I of this paper, the general theory for both response analysis and sensitivity analysis is described. In Part II, the theory is applied to a composite laminated beam problem.

## PART I. GENERAL THEORY

Nonlinear structural sensitivity analysis comprises three steps: the nonlinear structural response analysis, the response sensitivity analysis and the constraint sensitivity analysis. In this paper, the generalized Hooke's law is adopted as the elastic constitutive model and the rate-independent plasticity is chosen as the plastic constitutive model. Several techniques are available for response analysis, such as the Total Lagrangian formulation and the Updated Lagrangian formulation [1,4,5], which uses the load incrementation procedure to obtain increments in the response variables. A load incrementation procedure, which gives responses rather than their increments, is used in the present formulation to fit the class of nonlinear present problems. In the plastic range, the constitutive equations are a set of nonlinear differential equations. Several different numerical techniques have been proposed for the solution of these equations. Tsay *et al.* [1] proposed a linear approximation of the integration of the constitutive equations in the discussion of nonlinear sensitivity analysis. Lubliner [6] summarized the generalized Euler (predictor/corrector) method for viscoplasticity and rate-independent plasticity. In this paper, a higher order approximation of the integration of the rate equations is proposed. In the sensitivity analysis, the reference volume concept is to unify shape and nonshape design problems. The response sensitivity equations are obtained using the direct differentiation approach (DDA), in which design sensitivities of the equilibrium equations with respect to the design variables are

computed. A method of partial differentiation of the plastic constitutive equations, with respect to the design variable, is proposed which yields a set of linear differential equations in the partial derivatives of the stresses with respect to the design variables. Once the set of linear differential equations is solved, the sensitivity equations are used to determine the response sensitivities. Direct differentiation of the constraint functions with respect to the design variables and substitution of the response sensitivities result in the constraint sensitivities with respect to the design variables.

## CONTINUUM DEFORMATION

Consider a continuum initially occupying a domain  $C_0$  of volume  ${}^0V$  and bounded by the surface  ${}^0\Gamma$  (Figure 1). In this configuration, a material point is denoted  ${}^0\mathbf{x} = ({}^0x_1, {}^0x_2, {}^0x_3)^\top$  in a Cartesian coordinate system. At some time  $t$  (load level  $t$ ), the configuration deforms to a new configuration with a domain  $C_t$  of volume  ${}^tV$  and bounded by the surface  ${}^t\Gamma$  (Figure 1). The material point moves to a new position denoted  ${}^t\mathbf{x} = ({}^tx_1, {}^tx_2, {}^tx_3)^\top$  in another Cartesian coordinate system. The relation between  ${}^0\mathbf{x}$  and  ${}^t\mathbf{x}$  is described by the function

$${}^t\mathbf{x} = {}^t\mathbf{x}({}^0\mathbf{x}, t). \quad (\text{I.1})$$

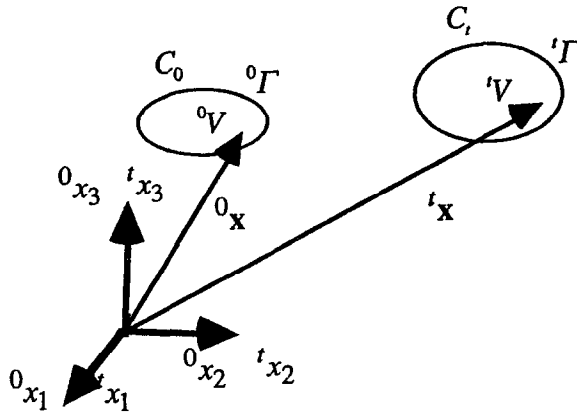


Figure 1. Deformation procedure.

Assuming that  ${}^t\mathbf{x}$  is continuously differentiable with respect to  ${}^0\mathbf{x}$ , the deformation gradient matrix of transformation from the initial configuration  $C_0$  to the deformed configuration  $C_t$  at  ${}^0\mathbf{x}$  is defined by  ${}^t_0\mathbf{F}({}^0\mathbf{x}, t)$ , whose Cartesian components are  ${}^t_0F_{ij} = \frac{\partial {}^tx_i}{\partial {}^0x_j}$ . The Jacobian determinant is  ${}^t_0J({}^0\mathbf{x}, t) = \det({}^t_0\mathbf{F}({}^0\mathbf{x}, t))$ .

Consider a material point  ${}^0\mathbf{x}$  and two neighboring points  ${}^0\mathbf{x}' = {}^0\mathbf{x} + d^0\mathbf{x}'$  and  ${}^0\mathbf{x}'' = {}^0\mathbf{x} + d^0\mathbf{x}''$ . The vector area of the triangle formed by the three points is denoted  $d^0\Gamma$ . At time  $t$ , the deformed positions of  ${}^0\mathbf{x}$ ,  ${}^0\mathbf{x}'$  and  ${}^0\mathbf{x}''$  are  ${}^t\mathbf{x}$ ,  ${}^t\mathbf{x}' = {}^t\mathbf{x} + {}^t_0\mathbf{F}d^0\mathbf{x}'$  and  ${}^t\mathbf{x}'' = {}^t\mathbf{x} + {}^t_0\mathbf{F}d^0\mathbf{x}''$ , respectively. The deformed area  $d^t\Gamma$  is given by

$$d^t\Gamma = {}^t_0J_\Gamma d^0\Gamma, \quad (\text{I.2})$$

where

$${}^t_0J_\Gamma = {}^t_0J \sqrt{\left(\frac{\partial {}^0x_i}{\partial {}^0x_1} {}^0n_i\right)^2 + \left(\frac{\partial {}^0x_i}{\partial {}^0x_2} {}^0n_i\right)^2 + \left(\frac{\partial {}^0x_i}{\partial {}^0x_3} {}^0n_i\right)^2}$$

and  ${}^0n_i$  ( $i = 1, 2, 3$ ) are the outward normal components of the initial surface  ${}^0\Gamma$ . If a fourth point is now defined by  ${}^0\mathbf{x}''' = {}^0\mathbf{x} + d^0\mathbf{x}'''$  and its deformed position by  ${}^t\mathbf{x}''' = {}^t\mathbf{x} + {}^t_0\mathbf{F}d^0\mathbf{x}'''$ , then the volume,  $d^0V$ , of the tetrahedron in the initial configuration and the deformed volume  $d^tV$  are related as follows

$$d^tV = {}^t_0J d^0V. \quad (\text{I.3})$$

## REFERENCE VOLUME CONCEPT

Define a reference configuration  $C_r$  with volume  ${}^rV$  and boundary  ${}^r\Gamma$  which does not deform during the design and loading processes. This concept of fixed reference volume is particularly useful in unifying the shape and nonshape design sensitivity analysis problems. Let  ${}^r\mathbf{x}$  be the position vector for each point in the fixed reference configuration  $C_r$ . For each design a unique mapping  ${}^0\mathbf{x} = {}^0\mathbf{x}({}^r\mathbf{x})$  is established that maps each point  ${}^r\mathbf{x}$  in  $C_r$  onto a material particle with coordinate  ${}^0\mathbf{x}$  in  $C_0$  and vice versa. This mapping will change with variations in the shape of the continuum, so that the material volume associated with  $C_r$  changes. However,  $C_r$  is invariant, so reference volume and surface area do not change with the design variations. Note that the mapping between the reference volume and the original configuration depends only on the design variation and is independent of the loading history. The differential volume and surface area in the initial configuration can be expressed in terms of the reference volume as  $d^0V = {}^0_rJ d^rV$  and  $d^0\Gamma = {}^0_rJ_\Gamma d^r\Gamma$ , respectively, where  ${}^0_rJ$  is the Jacobian determinant of transformation from the reference configuration to the initial configuration and

$${}^0_rJ_\Gamma = {}^0_rJ \sqrt{\left(\frac{\partial^r x_i}{\partial^0 x_1} {}^r n_i\right)^2 + \left(\frac{\partial^r x_i}{\partial^0 x_2} {}^r n_i\right)^2 + \left(\frac{\partial^r x_i}{\partial^0 x_3} {}^r n_i\right)^2},$$

where  ${}^r n_i (i = 1, 2, 3)$  are the outward normal components of reference surface  ${}^r\Gamma$ .

## PRINCIPLE OF VIRTUAL WORK

Equilibrium of a continuum can be described in two ways. The first is described by a set of differential equations and the second by a functional extremum. Mathematically, these two categories are equivalent to each other. In practice, the set of differential equations can be transformed to fit into the concrete classes of problems. The description of a functional extremum is used in the following formulation. The same procedure can also be used to describe the differential equations.

In the configuration  $C_t$ , any volume element  $d^tV$  experiences a body force  ${}^t\rho^t b d^tV$ , where  ${}^t\rho$  is the mass per unit volume at load level  $t$  and  ${}^t b$  is the body force per unit mass at load level  $t$ . Any oriented surface element  ${}^t n d^t\Gamma$  experiences a contact force  ${}^t \mathbf{t}({}^t \mathbf{n}) d^t\Gamma$ , where  ${}^t \mathbf{t}({}^t \mathbf{n})$  is the surface traction and  ${}^t \mathbf{n}$  is the unit outward normal on  ${}^t\Gamma$ . If  ${}^t \sigma_{ij}$  denotes the Cauchy stress tensor, then  ${}^t \mathbf{t}({}^t \mathbf{n}) = {}^t \sigma_{ij} {}^t n_j$ .

Consider two possible configurations  ${}^t \mathbf{x}$  and  ${}^t \mathbf{x} + \delta^t \mathbf{u}$ , where  $\delta^t \mathbf{u}$  is a virtual displacement field, and assume that the acceleration field vanishes identically. The principle of virtual work can be used to describe the equilibrium of a continuum at load level  $t$  as

$$\int_{{}^tV} {}^t \sigma_{ij} \delta^t \varepsilon_{ij} d^tV = \int_{{}^tV} {}^t \rho^t b_i \delta^t u_i d^tV + \int_{{}^t\Gamma} {}^t \sigma_{ij} {}^t n_j \delta^t u_i d^t\Gamma, \quad (I.4)$$

where  ${}^t \varepsilon_{ij} = (1/2) \left( \frac{\partial^t u_i}{\partial^t x_j} + \frac{\partial^t u_j}{\partial^t x_i} \right)$ . Equation (I.4) is solved using the Updated Lagrangian (UL) scheme [5]. Next, since reference volume concept is used, the above equation is transformed to the initial configuration ( $C_0$ ) as

$$\int_{{}^0V} {}^t \sigma_{ij} \delta^t \varepsilon_{ij} {}^t J d^0V = \int_{{}^0V} {}^0 \rho^t b_i \delta^t u_i d^0V + \int_{{}^0\Gamma} {}^t \sigma_{ij} {}^t n_j \delta^t u_i {}^t J_\Gamma d^r\Gamma. \quad (I.5)$$

Referring all the quantities in equation (I.5) to the reference volume, the equation is rewritten as

$$\int_{{}^rV} {}^t \sigma_{ij} \delta^t \varepsilon_{ij} {}^t J_r^0 J d^rV = \int_{{}^rV} {}^r \rho^t b_i \delta^t u_i d^rV + \int_{{}^r\Gamma} {}^t \sigma_{ij} {}^t n_j \delta^t u_i {}^t J_\Gamma^0 J_\Gamma d^r\Gamma. \quad (I.6)$$

Equation (I.6) is used in the sensitivity analysis.

## CONSTITUTIVE MODELS

Materials described by rate constitutive equations form an important class in structural mechanics because they describe phenomena like plasticity, creep, viscoelasticity and viscoplasticity. Thus, in this paper, a rate constitutive model is adopted to describe the plastic procedure. The kinematic formulation depends upon the assumptions made in describing the displacements, rotations and strains. The theory presented in this paper assumes a materially-nonlinear model with infinitesimal displacements and rotations. The formulation presented applies to generally anisotropic materials. The stress-strain relation of an elastoplastic material is often constructed on the basis of the following three basic concepts from the classical plasticity theory. These are: (a) yield criterion, (b) flow rule and (c) hardening rule. In addition, many elastoplastic models are based on the assumption that the infinitesimal strain at load level  $t$  can be decomposed into an elastic component  ${}^t\varepsilon_{ij}^e$  and a plastic component  ${}^t\varepsilon_{ij}^p$ , that is,  ${}^t\varepsilon_{ij} = {}^t\varepsilon_{ij}^e + {}^t\varepsilon_{ij}^p$ . The stress rates are related to the strain rates using Hooke's law as

$${}^t\dot{\sigma}_{ij} = C_{ijkl} {}^t\dot{\varepsilon}_{kl}^e = C_{ijkl} ({}^t\dot{\varepsilon}_{kl} - {}^t\dot{\varepsilon}_{kl}^p), \quad (I.7)$$

where  $C_{ijkl}$  are the elastic moduli of the structural material.

In the stress space, it is assumed that there exists an enclosed surface which is described by a yield surface,  $f({}^t\sigma_{ij}, {}^t\xi_1, \dots, {}^t\xi_n) = 0$ , where  ${}^t\xi_1, \dots, {}^t\xi_n$  are the internal variables at load level  $t$ . The plastic strain rate vanishes within that surface but not outside of it. An associated flow rule is adopted. Therefore, the plastic strain rates are written as

$${}^t\dot{\varepsilon}_{ij}^p = {}^t\dot{\lambda} \frac{\partial f}{\partial {}^t\sigma_{ij}}, \quad (I.8)$$

where  ${}^t\dot{\lambda}$  is determined by the condition that during the plastic deformation, the stresses remain on the yield surface, that is,

$$\frac{\partial f}{\partial {}^t\sigma_{ij}} {}^t\dot{\sigma}_{ij} + \frac{\partial f}{\partial {}^t\xi_k} {}^t\dot{\xi}_k = 0, \quad (I.9)$$

at load level  $t$ . Defining  ${}^tH {}^t\dot{\lambda} = -\frac{\partial f}{\partial {}^t\xi_k} {}^t\dot{\xi}_k$  (see [6]), equation (I.9) reduces to

$$\frac{\partial f}{\partial {}^t\sigma_{ij}} {}^t\dot{\sigma}_{ij} - {}^tH {}^t\dot{\lambda} = 0. \quad (I.10)$$

Substitution of equation (I.8) in (I.7) yields

$${}^t\dot{\sigma}_{ij} = C_{ijkl} \left( {}^t\dot{\varepsilon}_{kl} - {}^t\dot{\lambda} \frac{\partial f}{\partial {}^t\sigma_{kl}} \right). \quad (I.11)$$

Substituting equation (I.11) in (I.10),  ${}^t\dot{\lambda}$  is obtained

$${}^t\dot{\lambda} = \frac{\frac{\partial f}{\partial {}^t\sigma_{ij}} C_{ijkl} {}^t\dot{\varepsilon}_{kl}}{{}^tH + \frac{\partial f}{\partial {}^t\sigma_{ij}} C_{ijkl} \frac{\partial f}{\partial {}^t\sigma_{kl}}}. \quad (I.12)$$

The hardening property  ${}^tH$  may be related to the plastic modulus  $\frac{d^t\sigma}{d^t\varepsilon^p}$  obtained in a simple tension test [5-7]. Substituting equation (I.12) in equation (I.11), the stress-strain rate equations are obtained.

$${}^t\dot{\sigma}_{ij} = {}^tP_{ijkl} {}^t\dot{\varepsilon}_{kl}, \quad (I.13)$$

where

$${}^tP_{ijkl} = C_{ijkl} - \frac{C_{ijmn} \frac{\partial f}{\partial {}^t\sigma_{mn}} \frac{\partial f}{\partial {}^t\sigma_{pq}} C_{pqkl}}{{}^tH + \frac{\partial f}{\partial {}^t\sigma_{pq}} C_{pqst} \frac{\partial f}{\partial {}^t\sigma_{st}}}, \quad (I.14)$$

represent the instantaneous elastoplastic stiffnesses. Note that  ${}^tP_{ijkl}$  are functions of the stresses, the internal variables and the material constants.

The presence of internal variables in the constitutive relations requires additional constitutive equations, that is, the equations of evolution. Among the three quantities  $\sigma_{ij}$ ,  $\varepsilon_{ij}$  and  $\xi_r$ , only two are independent. In this paper,  $\varepsilon_{ij}$  and  $\xi_r$  are used as independent variables and  $\sigma_{ij}$  can be expressed in terms of the remaining two variables,  $\varepsilon_{ij}$  and  $\xi_r$ . The quantities  $\sigma_{ij}$  and  $\xi_r$  can be used as independent variables and  $\varepsilon_{ij}$  can be expressed in terms of  $\sigma_{ij}$  and  $\xi_r$  (see [6]). The equations of evolution are defined as

$${}^t\dot{\xi}_r = g_r({}^t\sigma, {}^t\xi), \quad (\text{I.15})$$

for the  $r^{\text{th}}$  internal variable  $r = (1, \dots, n)$ . For rate-independent plasticity, the above can be written as

$${}^t\dot{\xi}_r = {}^t\dot{\lambda}h_r({}^t\sigma, {}^t\xi) = {}^tQ_{rkl}{}^t\dot{\varepsilon}_{kl}, \quad (\text{I.16})$$

where

$${}^tQ_{rkl} = \frac{h_r \frac{\partial f}{\partial \sigma_{ij}} C_{ijkl}}{{}^tH + \frac{\partial f}{\partial \sigma_{ij}} C_{ijmn} \frac{\partial f}{\partial \sigma_{mn}}} \quad (\text{I.17})$$

are functions of the stresses, the internal variables and the material constants. Equations (I.13) and (I.16) are the rate-independent constitutive equations of plasticity for composite materials.

The above constitutive equations are for loading. With unloading, changes occur only in the elastic strain components. The elastic strain components are related to the stress components by the generalized Hooke's law [8]. The plastic strain components do not change and are equal to the respective plastic strains attained at the initial instant of unloading.

## HIGHER ORDER APPROXIMATION OF RATE CONSTITUTIVE EQUATIONS

In the plastic range, the constitutive equations are a set of nonlinear differential equations with the elastoplastic yield stresses at the yield points as the initial conditions. Numerical solution of this initial value problem for each load level is CPU intensive. Several numerical techniques have been presented for the time integration of the differential equation arising in elastoplastic problems. Tsay et al. [1] proposed a linear approximation of the integration of the constitutive equations in the discussion of nonlinear sensitivity analysis. Lubliner [6] summarized the generalized Euler (predictor/corrector) method for viscoplasticity and rate-independent plasticity. These techniques are basically based on the linear approaches. However, in many cases the constitutive equations are continuously-higher-order differentiable with respect to the parameters in the plastic range. Therefore, a higher order approximation technique of the integration of the rate constitutive equations is proposed for these kinds of problems. Assume that the responses have been solved at load level  $\tau$ . For the following load level  $t$ , integration of equation (I.13) from the load level  $\tau$  to the load level  $t$  yields

$${}^t\sigma_{ij} = \tau\sigma_{ij} + \int_{\tau\varepsilon_{kl}}^{t\varepsilon_{kl}} \zeta P_{ijkl} d^{\zeta}\varepsilon_{kl}. \quad (\text{I.18})$$

The above is approximated as follows:

$${}^t\sigma_{ij} = \tau\sigma_{ij} + \tau P_{ijkl}({}^t\varepsilon_{kl} - \tau\varepsilon_{kl}) + \frac{1}{2} \frac{\partial \tau P_{ijkl}}{\partial \tau \varepsilon_{mn}} ({}^t\varepsilon_{kl} - \tau\varepsilon_{kl}) ({}^t\varepsilon_{mn} - \tau\varepsilon_{mn}), \quad (\text{I.19})$$

where  $\frac{\partial \tau P_{ijkl}}{\partial \tau \varepsilon_{mn}}$  is calculated as

$$\frac{\partial \tau P_{ijkl}}{\partial \tau \varepsilon_{mn}} = \frac{\partial \tau P_{ijkl}}{\partial \tau \sigma_{pq}} \tau P_{pqmn} + \frac{\partial \tau P_{ijkl}}{\partial \tau \xi_r} \tau Q_{rnm}. \quad (\text{I.20})$$

Integration of equation (I.16) from the previous load level  $\tau$  to the current load level  $t$  yields

$${}^t\xi_r = \tau\xi_r + \int_{\tau\varepsilon_{kl}}^{t\varepsilon_{kl}} \zeta Q_{rkl} d^{\zeta}\varepsilon_{kl}. \quad (\text{I.21})$$

The above is approximated as

$${}^t\xi_r = \tau\xi_r + \tau Q_{rkl}({}^t\varepsilon_{kl} - \tau\varepsilon_{kl}) + \frac{1}{2} \frac{\partial \tau Q_{rkl}}{\partial \tau \varepsilon_{mn}} ({}^t\varepsilon_{kl} - \tau\varepsilon_{kl}) ({}^t\varepsilon_{mn} - \tau\varepsilon_{mn}), \quad (\text{I.22})$$

where  $\frac{\partial \tau Q_{rkl}}{\partial \tau \varepsilon_{mn}}$  is calculated as

$$\frac{\partial \tau Q_{rkl}}{\partial \tau \varepsilon_{mn}} = \frac{\partial \tau Q_{rkl}}{\partial \tau \sigma_{pq}} \tau P_{pqmn} + \frac{\partial \tau Q_{rkl}}{\partial \tau \xi_s} \tau Q_{smn}. \quad (\text{I.23})$$

Equations (I.19) and (I.22) represent the second order approximation of the constitutive equations in the strains  ${}^t\varepsilon_{kl}$ . Numerically, the linear approximation has first order accuracy in strain difference, that is,  $o({}^t\varepsilon_{kl} - \tau\varepsilon_{kl})$ , whereas the second approximation and the generalized Euler method have second order accuracy in strain difference [8], that is,  $o({}^t\varepsilon_{kl} - \tau\varepsilon_{kl})({}^t\varepsilon_{mn} - \tau\varepsilon_{mn})$ . As long as the higher order derivatives of  $\tau P_{ijkl}$  and  $\tau Q_{rkl}$  with respect to the strains exist, the higher order approximation of the constitutive equations can be obtained using the Taylor expansions of the integrations in equations (I.18) and (I.21).

## DIRECT DIFFERENTIATION APPROACH (DDA)

The direct differentiation approach, also known as the direct variational method, is an effective approach for calculating the response sensitivities and this approach is used in this paper to calculate the sensitivities, with respect to the design variables. The procedure involves taking design variations of the equilibrium equations and the constitutive equations [1,4]. Using this method, a technique for the integration of the variation of the rate constitutive equation is required to find the response sensitivities [4]. To avoid the integration of the variations of the constitutive equations, a new procedure called the design partial differentiation of the constitutive equations is presented in this paper. This procedure is as follows. Let  $\mathbf{d} = (d_1, \dots, d_p)^\top$  denote the design variable vector, where  $p$  is the total number of design variables. Assume that at load level  $t$ , the responses have been solved from the response analysis. Note that in the equilibrium equation (I.6), the quantities  ${}^0J, {}^r\rho$  and  ${}^0J_\Gamma$  are functions of design variables only, the quantities  ${}^t_0J, {}^t b_i, {}^t n_j$  and  ${}^t_0J_\Gamma$  are functions of displacements, internal variables and design variables and the quantities  ${}^t\sigma_{ij}$  are functions of strains, internal variables and design variables. For  ${}^t\sigma_{ij}({}^t\varepsilon_{kl}, {}^t\xi_r, \mathbf{d})$ , where  ${}^t\varepsilon_{kl}$  and  ${}^t\xi_r$  are the two independent variables, using the chain rule of differentiation yields

$$\frac{d^t\sigma_{ij}}{dd_m} = \frac{\partial^t\sigma_{ij}}{\partial^t\varepsilon_{pq}} \frac{d^t\varepsilon_{pq}}{dd_m} + \frac{\partial^t\sigma_{ij}}{\partial^t\xi_r} \frac{d^t\xi_r}{dd_m} + \frac{\partial^t\sigma_{ij}}{\partial d_m}. \quad (\text{I.24})$$

Using the chain rule for the derivatives of the quantities  ${}^t_0J, {}^t b_i, {}^t n_j$  and  ${}^t_0J_\Gamma$ , differentiation of equation (I.6) with respect to the design variable  $d_m$  yields

$$\begin{aligned} & \int_{rV} \left\{ \left[ \left( \frac{\partial^t\sigma_{ij}}{\partial^t\varepsilon_{pq}} \frac{d^t\varepsilon_{pq}}{dd_m} + \frac{\partial^t\sigma_{ij}}{\partial^t\xi_r} \frac{d^t\xi_r}{dd_m} + \frac{\partial^t\sigma_{ij}}{\partial d_m} \right) \delta^t\varepsilon_{ij} + {}^t\sigma_{ij} \delta \left( \frac{d^t\varepsilon_{ij}}{dd_m} \right) \right] {}^t_0J_r^0J \right\} d^rV \\ & + \int_{rV} \left\{ {}^t\sigma_{ij} \delta^t\varepsilon_{ij} \left[ \left( \frac{\partial^t_0J}{\partial^t u_i} \frac{d^t u_i}{dd_m} + \frac{\partial^t_0J}{\partial^t \xi_r} \frac{d^t \xi_r}{dd_m} + \frac{\partial^t_0J}{\partial d_m} \right) {}^0J + {}^t_0J \frac{d^0_0J}{dd_m} \right] \right\} d^rV \\ & = \int_{rV} \left\{ \frac{d^r\rho}{dd_m} {}^t b_i \delta^t u_i + {}^r\rho \left[ \left( \frac{\partial^t b_i}{\partial^t u_j} \frac{d^t u_j}{dd_m} + \frac{\partial^t b_i}{\partial^t \xi_r} \frac{d^t \xi_r}{dd_m} + \frac{\partial^t b_i}{\partial d_m} \right) \delta^t u_i + {}^t b_i \delta \left( \frac{d^t u_i}{dd_m} \right) \right] \right\} d^rV \\ & + \int_{r\Gamma} \left\{ \left[ \left( \frac{\partial^t\sigma_{ij}}{\partial^t\varepsilon_{pq}} \frac{d^t\varepsilon_{pq}}{dd_m} + \frac{\partial^t\sigma_{ij}}{\partial^t\xi_r} \frac{d^t\xi_r}{dd_m} + \frac{\partial^t\sigma_{ij}}{\partial d_m} \right) {}^t n_j + {}^t\sigma_{ij} \left( \frac{\partial^t n_j}{\partial^t u_k} \frac{d^t u_k}{dd_m} + \frac{\partial^t n_j}{\partial^t \xi_r} \frac{d^t \xi_r}{dd_m} + \frac{\partial^t n_j}{\partial d_m} \right) \right] \right. \\ & \quad \times \delta^t u_i {}^t_0J_\Gamma^0J_\Gamma + {}^t\sigma_{ij} {}^t n_j \\ & \quad \left. \times \left[ \delta \left( \frac{d^t u_i}{dd_m} \right) {}^t_0J_\Gamma^0J_\Gamma + \delta^t u_i \left( \left( \frac{\partial^t_0J_\Gamma}{\partial^t u_k} \frac{d^t u_k}{dd_m} + \frac{\partial^t_0J_\Gamma}{\partial^t \xi_r} \frac{d^t \xi_r}{dd_m} + \frac{\partial^t_0J_\Gamma}{\partial d_m} \right) {}^0J_\Gamma + {}^t_0J_\Gamma \frac{d^0_0J_\Gamma}{dd_m} \right) \right] \right\} d^r\Gamma. \quad (\text{I.25}) \end{aligned}$$

In equation (I.25), the quantities  $\frac{\partial_0^t J}{\partial^t u_i}$ ,  $\frac{\partial_0^t J}{\partial^t \xi_r}$ ,  $\frac{\partial_0^t J}{\partial d_m}$ ,  $\frac{d_0^t J}{dd_m}$ ,  $\frac{d^r \rho}{dd_m}$ ,  $\frac{\partial^t b_i}{\partial^t u_j}$ ,  $\frac{\partial^t b_i}{\partial^t \xi_r}$ ,  $\frac{\partial^t b_i}{\partial d_m}$ ,  $\frac{\partial^t n_i}{\partial^t u_k}$ ,  $\frac{\partial^t n_i}{\partial^t \xi_r}$ ,  $\frac{\partial^t n_i}{\partial d_m}$ ,  $\frac{\partial_0^t J_\Gamma}{\partial^t u_k}$ ,  $\frac{\partial_0^t J_\Gamma}{\partial^t \xi_r}$ ,  $\frac{\partial_0^t J_\Gamma}{\partial d_m}$  and  $\frac{d_0^t J_\Gamma}{dd_m}$  are known from the displacements, the internal variables and the design variables; the quantities  $\frac{\partial^t \sigma_{ij}}{\partial^t \varepsilon_{pq}}$  and  $\frac{\partial^t \sigma_{ij}}{\partial^t \xi_r}$  can be calculated from the constitutive equations, and  $\frac{d^t \varepsilon_{pq}}{dd_m}$  can be expressed linearly in terms of  $\frac{d^t u_i}{dd_m}$ . In the elastic range, since  ${}^t \sigma_{ij}$  are explicit functions of the design variable  $d_m$ , the quantities  $\frac{\partial^t \sigma_{ij}}{\partial d_m}$  can be obtained by direct differentiation of their relations. Furthermore, since the internal variables vanish in the elastic range, so do their sensitivities. Therefore, the only unknowns are the quantities  $\frac{d^t u_i}{dd_m}$ , which can be solved for using equation (I.25). In the plastic range, the quantities  $\frac{\partial^t \sigma_{ij}}{\partial d_m}$  and  $\frac{d^t \xi_r}{dd_m}$  are unknown since  ${}^t \sigma_{ij}$  and  ${}^t \xi_r$  cannot be expressed explicitly by the design variable  $d_m$  (they are related by the constitutive equations which are a set of nonlinear differential equations). Thus, in the plastic range the unknowns in equation (I.25) are  $\frac{\partial^t \sigma_{ij}}{\partial d_m}$ ,  $\frac{d^t \xi_r}{dd_m}$ , and  $\frac{d^t u_i}{dd_m}$ . To solve the sensitivity equations, supplementary equations are required. The following section describes a procedure to get the supplementary equations in  $\frac{\partial^t \sigma_{ij}}{\partial d_m}$ ,  $\frac{d^t \xi_r}{dd_m}$  and  $\frac{d^t u_i}{dd_m}$  in the plastic range.

## DESIGN PARTIAL DIFFERENTIATION (DPD) OF CONSTITUTIVE EQUATIONS

Keeping the displacements and the internal variables fixed, partial differentiation of the constitutive equations (I.13) with respect to the design variable  $d_m$  yields

$$d \left( \frac{\partial^t \sigma_{ij}}{\partial d_m} \right) = \left( \frac{\partial^t P_{ijkl}}{\partial^t \sigma_{pq}} \frac{\partial^t \sigma_{pq}}{\partial d_m} + \frac{\partial^t P_{ijkl}}{\partial d_m} \right) d^t \varepsilon_{kl}. \quad (\text{I.26})$$

Derivative of equation (I.16) with respect to  $d_m$  yields

$$d \left( \frac{d^t \xi_r}{dd_m} \right) = \left[ \frac{\partial^t Q_{rkl}}{\partial^t \sigma_{pq}} \left( \frac{\partial^t \sigma_{pq}}{\partial^t \varepsilon_{ij}} \frac{d^t \varepsilon_{ij}}{dd_m} + \frac{\partial^t \sigma_{pq}}{\partial^t \xi_r} \frac{d^t \xi_r}{dd_m} + \frac{\partial^t \sigma_{pq}}{\partial d_m} \right) + \frac{\partial^t Q_{rkl}}{\partial^t \xi_s} \frac{d^t \xi_s}{dd_m} + \frac{\partial^t Q_{rkl}}{\partial d_m} \right] d^t \varepsilon_{kl} + {}^t Q_{rkl} d \left( \frac{d^t \varepsilon_{kl}}{dd_m} \right). \quad (\text{I.27})$$

In the above equations, the quantities  $\frac{\partial^t P_{ijkl}}{\partial^t \sigma_{pq}}$ ,  $\frac{\partial^t P_{ijkl}}{\partial d_m}$ ,  $\frac{\partial^t Q_{rkl}}{\partial^t \sigma_{pq}}$ ,  $\frac{\partial^t Q_{rkl}}{\partial^t \xi_r}$  and  $\frac{\partial^t Q_{rkl}}{\partial d_m}$  can be obtained from the definitions of  ${}^t P_{ijkl}$  and  ${}^t Q_{rkl}$ , respectively. The quantities  $\frac{d^t \varepsilon_{kl}}{dd_m}$  are linear functions of  $\frac{d^t u_i}{dd_m}$ . Therefore, equations (I.26) and (I.27) represent a set of linear differential equations in  $\frac{\partial^t \sigma_{ij}}{\partial d_m}$ ,  $\frac{d^t \xi_r}{dd_m}$ , and  $\frac{d^t u_i}{dd_m}$ . Their initial values can be obtained by differentiating the initial yield stresses and the initial internal variables with respect to the design variable  $d_m$ . Note that the stresses are functions of  ${}^t \varepsilon_{ij}$ ,  ${}^t \xi_r$  and  $\mathbf{d}$  and the internal variables are functions of  $\mathbf{d}$ , that is,  ${}^t \sigma_{ij}({}^t \varepsilon_{kl}, {}^t \xi_r, \mathbf{d})$  and  ${}^t \xi_r(\mathbf{d})$ . Thus, at the yield point the yield stresses and the initial internal variables can be written as  ${}_0 \sigma_{ij}({}_0 \varepsilon_{kl}, {}_0 \xi_r, \mathbf{d})$  and  ${}_0 \xi_r(\mathbf{d})$ , where  ${}_0 \varepsilon_{kl}$  is the yield strain tensor and  ${}_0 \xi_r$  is the initial internal variable vector which are determined from the elastic solutions and the yield function. Denoting  ${}_0 A_{ij}$  and  ${}_0 B_r$  the values of the yield stresses and the internal variables, respectively, the yield stresses  ${}_0 \sigma_{ij}$  and the initial internal variables  ${}_0 \xi_r$  can be expressed as

$${}_0 \sigma_{ij}({}_0 \varepsilon_{kl}, {}_0 \xi_r, \mathbf{d}) = {}_0 A_{ij}, \quad (\text{I.28})$$

$${}_0 \xi_r(\mathbf{d}) = {}_0 B_r. \quad (\text{I.29})$$

Derivatives of equations (I.28) and (I.29) with respect to the design variable  $d_m$  yield

$$\frac{\partial_0 \sigma_{ij}}{\partial d_m} = \frac{d_0 A_{ij}}{dd_m} - \left( \frac{\partial_0 \sigma_{ij}}{\partial_0 \varepsilon_{pq}} \frac{d_0 \varepsilon_{pq}}{dd_m} + \frac{\partial_0 \sigma_{ij}}{\partial_0 \xi_s} \frac{d_0 \xi_s}{dd_m} \right), \quad (\text{I.30})$$

$$\frac{d_0 \xi_r}{dd_m} = \frac{d_0 B_r}{dd_m}. \quad (\text{I.31})$$

The above equations represent the initial conditions of the linear differential equations (I.26) and (I.27). The response sensitivities can be obtained by combining equations (I.25)–(I.27) along with the initial conditions, equations (I.30) and (I.31). This linear problem is relatively easy to solve numerically compared to the integration procedure of the variations of the constitutive equations used in the traditional DDA. This also overcomes the problem of the discontinuities of design sensitivities at the material yield points by separating the sensitivity analysis in the plastic range from that in the elastic range.

## CONSTRAINT SENSITIVITY

The problem is to find design sensitivities of quantities, such as displacements, stresses and strains of a nonlinear structural system at load level  $t$ . Such constraints may be represented by the general functional

$$\Phi = \int_{\circ V(\mathbf{d})} G({}^t\sigma_{ij}, {}^t\varepsilon_{ij}, {}^t\xi_r, {}^t u_i, \mathbf{d}) d^0V + \int_{\circ\Gamma(\mathbf{d})} h({}^t\sigma_{ij}, {}^t\xi_r, {}^t u_i, \mathbf{d}) d^0\Gamma. \quad (\text{I.32})$$

The constraints can also be represented by ordinary functions. Further, the following discussion focused on the functional (I.32) can also be applied to the ordinary functions. Referring all the quantities to the reference volume, equation (I.32) becomes

$$\Phi = \int_{\circ V(\mathbf{d})} G({}^t\sigma_{ij}, {}^t\varepsilon_{ij}, {}^t\xi_r, {}^t u_i, \mathbf{d})_r^0 J d^rV + \int_{\circ\Gamma(\mathbf{d})} h({}^t\sigma_{ij}, {}^t\xi_r, {}^t u_i, \mathbf{d})_r^0 J_\Gamma d^r\Gamma. \quad (\text{I.33})$$

The sensitivity of the constraint with respect to the design variable  $d_m$  is

$$\begin{aligned} \frac{\partial\Phi}{\partial d_m} = & \int_{\circ V(\mathbf{d})} \left[ \left( \frac{\partial G}{\partial {}^t\sigma_{ij}} \frac{d^t\sigma_{ij}}{dd_m} + \frac{\partial G}{\partial {}^t\varepsilon_{ij}} \frac{d^t\varepsilon_{ij}}{dd_m} + \frac{\partial G}{\partial {}^t\xi_r} \frac{d^t\xi_r}{dd_m} + \frac{\partial G}{\partial {}^t u_i} \frac{d^t u_i}{dd_m} + \frac{\partial G}{\partial d_m} \right)_r^0 J + G \frac{d_r^0 J}{dd_m} \right] d^rV \\ & + \int_{\circ\Gamma(\mathbf{d})} \left[ \left( \frac{\partial h}{\partial {}^t\sigma_{ij}} \frac{d^t\sigma_{ij}}{dd_m} + \frac{\partial h}{\partial {}^t\xi_r} \frac{d^t\xi_r}{dd_m} + \frac{\partial h}{\partial {}^t u_i} \frac{d^t u_i}{dd_m} + \frac{\partial h}{\partial d_m} \right)_r^0 J_\Gamma + h \frac{d_r^0 J_\Gamma}{dd_m} \right] d^r\Gamma. \end{aligned} \quad (\text{I.34})$$

Note that in the above equation, the quantities  $\frac{\partial G}{\partial {}^t\sigma_{ij}}$ ,  $\frac{\partial G}{\partial {}^t\varepsilon_{ij}}$ ,  $\frac{\partial G}{\partial {}^t\xi_r}$ ,  $\frac{\partial G}{\partial {}^t u_i}$  and  $\frac{\partial G}{\partial d_m}$  can be obtained from the explicit function  $G({}^t\sigma_{ij}, {}^t\varepsilon_{ij}, {}^t\xi_r, {}^t u_i, \mathbf{d})$ , the quantities  $\frac{\partial h}{\partial {}^t\sigma_{ij}}$ ,  $\frac{\partial h}{\partial {}^t\xi_r}$ ,  $\frac{\partial h}{\partial {}^t u_i}$  and  $\frac{\partial h}{\partial d_m}$  can be obtained from the explicit function  $h({}^t\sigma_{ij}, {}^t\xi_r, {}^t u_i, \mathbf{d})$  and the terms  $\frac{d_r^0 J}{dd_m}$  and  $\frac{d_r^0 J_\Gamma}{dd_m}$  can be directly calculated from  ${}^0_r J(\mathbf{d})$  and  ${}^0_r J_\Gamma(\mathbf{d})$ . The quantities  $\frac{\partial {}^t\sigma_{ij}}{\partial d_m}$ ,  $\frac{d^t\varepsilon_{ij}}{dd_m}$ ,  $\frac{d^t\xi_r}{dd_m}$ , and  $\frac{d^t u_i}{dd_m}$  can be obtained from the response sensitivity analysis. Therefore, (I.34) can be used to calculate the design sensitivities of the constraints.

## PART II. APPLICATION TO COMPOSITE LAMINATED BEAM

The general theory discussed in Part I is applied to a composite beam undergoing pure bending. A materially-nonlinear model is chosen to represent the rate constitutive equations. The Tsai-Hill theory is adopted as the yield criterion. In the response analysis, the curvatures and stresses of the beam are calculated. In the sensitivity analysis, the sensitivity of the curvatures and stresses with respect to ply angle are calculated by the direct differentiation approach (DDA) and the central finite difference approach (CFDA). The details of the analysis procedure, as applied to composites, are outlined in the following sections. In the following derivations, it must be noted that the summation is no longer used.

## MODELING ASSUMPTIONS

Consider a composite laminated beam undergoing pure bending. The beam is made of an orthotropic laminate of  $2k$  antisymmetrically stacked layers, each of which possesses different mechanical properties, thickness  $T_i$  and ply orientations  $\theta_i$  (Figure 2a). The cross section of the beam is rectangular with width  $b$  and height  $h$ . The following discussions are based on the assumptions of plane stress. It is also assumed that the materials possess identical properties in tension and in compression.

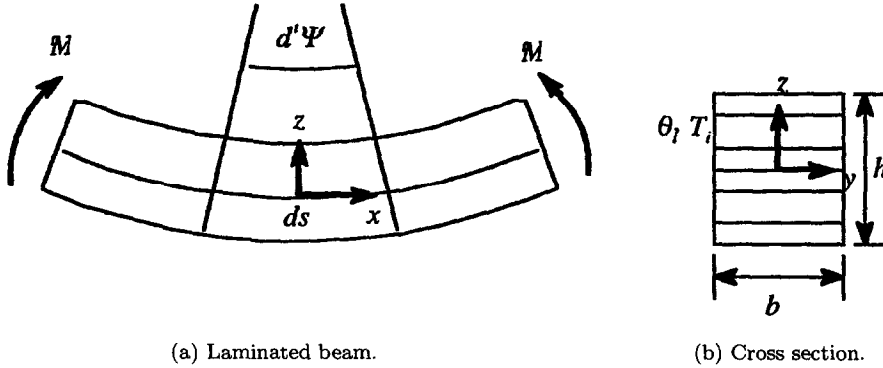


Figure 2. Laminated beam under pure bending.

## STRAIN ANALYSIS

Since the material is assumed to have identical properties in tension and compression, the middle surface of the beam is neither extended nor shortened. Considering a differential segment  $ds$  along the deflection curve (Figure 2a), the strain along the  $x$ -direction, at a point  $z$  and at load level  $t$  is

$${}^t\varepsilon_x = -z \frac{d^t\Psi}{ds}, \quad (\text{II.1})$$

where  $x, y$  represent the reference axes (Figure 2b),  ${}^t\Psi$  is the rotation angle of the section and  $\frac{d^t\Psi}{ds}$  is the curvature of the deflection curve. Defining  ${}^t\varphi = \frac{d^t\Psi}{ds}$ , equation (II.1) is written as

$${}^t\varepsilon_x = -z {}^t\varphi. \quad (\text{II.2})$$

Since the strain in the  $y$ -direction and the shear strain in the  $x$ - $y$  plane are very small compared to the strain in the direction  $x$ , they are assumed to be negligible in the following analysis, that is,  ${}^t\varepsilon_y = 0$  and  ${}^t\gamma_{xy} = 0$ . Therefore, the strains in the  $i^{\text{th}}$  layer in the principal material directions at load level  $t$  are calculated as

$$\begin{aligned} {}^t\varepsilon_1^i &= -z {}^t\varphi (\cos \theta_i)^2, \\ {}^t\varepsilon_2^i &= -z {}^t\varphi (\sin \theta_i)^2, \\ {}^t\gamma_{12}^i &= -z {}^t\varphi \sin 2\theta_i, \end{aligned} \quad (\text{II.3})$$

where  $z$  is in the interval of  $\left[ \sum_{j=0}^{i-1} T_j, \sum_{j=0}^i T_j \right]$  (where  $T_0 = 0$ ).

## CONSTITUTIVE EQUATIONS

The material model adopts the Tsai-Hill theory [9], in which the derivation of the anisotropic parameters depends on the initial yield surface and subsequently on the histories of the plastic deformation. The strain hardening is assumed to be isotropic, which at progressively higher stresses exhibits uniform expansion of the initial yield surface. For the  $i^{\text{th}}$  layer of the beam, the yield surface at load level  $t$  is given by

$$f({}^t\sigma_1^i, {}^t\sigma_2^i, {}^t\tau_{12}^i) = \frac{({}^t\sigma_1^i)^2}{({}^tX_i)^2} - \frac{{}^t\sigma_1^i {}^t\sigma_2^i}{({}^tX_i)^2} + \frac{({}^t\sigma_2^i)^2}{({}^tY_i)^2} + \frac{({}^t\tau_{12}^i)^2}{({}^tS_i)^2} - 1 = 0, \quad (\text{II.4})$$

where  ${}^tX_i$  is the longitudinal strength at load level  $t$ ,  ${}^tY_i$  is the transverse strength at load level  $t$  and  ${}^tS_i$  is the shear strength at load level  $t$ . In this paper, an elastic-perfectly plastic model is assumed. This implies that the strengths are constant and are equal to their initial values.

Therefore, the hardening property  ${}^tH = 0$ . In the elastic range, the strain is related to the stress by Hooke's law as

$$\begin{Bmatrix} {}^t\sigma_1^i \\ {}^t\sigma_2^i \\ {}^t\tau_{12}^i \end{Bmatrix} = \begin{bmatrix} C_{11}^i & C_{12}^i & 0 \\ C_{12}^i & C_{22}^i & 0 \\ 0 & 0 & C_{66}^i \end{bmatrix} \begin{Bmatrix} {}^t\varepsilon_1^i \\ {}^t\varepsilon_2^i \\ {}^t\gamma_{12}^i \end{Bmatrix}, \quad (\text{II.5})$$

where  $C_{11}^i = \frac{E_1^i}{1-\nu_{12}^i\nu_{21}^i}$ ,  $C_{12}^i = \frac{\nu_{12}^i E_2^i}{1-\nu_{12}^i\nu_{21}^i}$ ,  $C_{22}^i = \frac{E_2^i}{1-\nu_{12}^i\nu_{21}^i}$  and  $C_{66}^i = G_{12}^i$  and  $E_1^i, E_2^i$  are the Young's moduli,  $\nu_{12}^i, \nu_{21}^i$  are the Poisson's ratios and  $G_{12}^i$  is the shear modulus of the  $i^{\text{th}}$  layer.

The yield position  $z_0^i$  of the  $i^{\text{th}}$  layer can be obtained from the yield surface equation (II.4). Substitution of equations (II.3) and (II.5) in equation (II.4) yields

$$z_0^i = \frac{1}{{}^t\varphi \sqrt{\frac{(C_1^i)^2}{(X_i)^2} - \frac{C_2^i C_3^i}{(X_i)^2} + \frac{(C_2^i)^2}{(Y_i)^2} + \frac{(C_3^i)^2}{(S_i)^2}}}, \quad (\text{II.6a})$$

where

$$\begin{aligned} C_1^i &= C_{11}^i (\cos \theta_i)^2 + C_{12}^i (\sin \theta_i)^2, \\ C_2^i &= C_{12}^i (\cos \theta_i)^2 + C_{22}^i (\sin \theta_i)^2, \\ C_3^i &= C_{66}^i \sin 2\theta_i. \end{aligned} \quad (\text{II.6b})$$

For a position  $z$  on the  $i^{\text{th}}$  layer, if  $z \leq z_0^i$  material is elastic, otherwise it is plastic.

Substituting equation (II.3) in equation (II.5), the elastic constitutive equations (II.5) reduce to

$$\begin{aligned} {}^t\sigma_1^i &= -z {}^t\varphi [C_{11}^i (\cos \theta_i)^2 + C_{12}^i (\sin \theta_i)^2], \\ {}^t\sigma_2^i &= -z {}^t\varphi [C_{12}^i (\cos \theta_i)^2 + C_{22}^i (\sin \theta_i)^2], \\ {}^t\tau_{12}^i &= z {}^t\varphi C_{66}^i \sin 2\theta_i. \end{aligned} \quad (\text{II.7})$$

Using equations (II.3)–(II.5), the plastic constitutive equations (I.13) are written as

$$\begin{aligned} \frac{d^t\sigma_1^i}{d^t\varphi} &= z \left[ -{}^tA_{11}^i (\cos \theta_i)^2 - {}^tA_{12}^i (\sin \theta_i)^2 + \frac{1}{2} {}^tA_{13}^i \sin 2\theta_i \right], \\ \frac{d^t\sigma_2^i}{d^t\varphi} &= z \left[ -{}^tA_{12}^i (\cos \theta_i)^2 - {}^tA_{22}^i (\sin \theta_i)^2 + \frac{1}{2} {}^tA_{23}^i \sin 2\theta_i \right], \\ \frac{d^t\tau_{12}^i}{d^t\varphi} &= z \left[ -{}^tA_{13}^i (\cos \theta_i)^2 - {}^tA_{23}^i (\sin \theta_i)^2 + \frac{1}{2} {}^tA_{33}^i \sin 2\theta_i \right], \end{aligned} \quad (\text{II.8a})$$

where

$$\begin{aligned} {}^tA_{11}^i &= C_{11}^i - \frac{{}^tB_{11}^i}{{}^tC^i}, \quad {}^tA_{12}^i = C_{12}^i - \frac{{}^tB_{12}^i}{{}^tC^i}, \quad {}^tA_{13}^i = -\frac{{}^tB_{13}^i}{{}^tC^i}, \\ {}^tA_{22}^i &= C_{22}^i - \frac{{}^tB_{22}^i}{{}^tC^i}, \quad {}^tA_{23}^i = -\frac{{}^tB_{23}^i}{{}^tC^i}, \quad {}^tA_{33}^i = 2C_{66}^i - \frac{{}^tB_{33}^i}{{}^tC^i}, \\ {}^tB_{11}^i &= (C_{11}^i)^2 ({}^tD_1^i)^2 + 2C_{11}^i C_{12}^i {}^tD_1^i {}^tD_2^i + (C_{12}^i)^2 ({}^tD_2^i)^2, \\ {}^tB_{12}^i &= C_{11}^i C_{12}^i ({}^tD_1^i)^2 + [(C_{12}^i)^2 + C_{11}^i C_{22}^i] {}^tD_1^i {}^tD_2^i + C_{12}^i C_{22}^i ({}^tD_2^i)^2, \\ {}^tB_{13}^i &= 2C_{11}^i C_{66}^i {}^tD_1^i {}^tD_3^i + 2C_{12}^i C_{66}^i {}^tD_2^i {}^tD_3^i, \\ {}^tB_{22}^i &= (C_{12}^i)^2 ({}^tD_1^i)^2 + 2C_{12}^i C_{22}^i {}^tD_1^i {}^tD_2^i + (C_{22}^i)^2 ({}^tD_2^i)^2, \\ {}^tB_{23}^i &= 2C_{12}^i C_{66}^i {}^tD_1^i {}^tD_3^i + 2C_{22}^i C_{66}^i {}^tD_2^i {}^tD_3^i, \\ {}^tB_{33}^i &= 4(C_{66}^i)^2 ({}^tD_3^i)^2, \\ {}^tC^i &= {}^tH^i + C_{11}^i ({}^tD_1^i)^2 + 2C_{12}^i {}^tD_1^i {}^tD_2^i + C_{22}^i ({}^tD_2^i)^2 + 2C_{66}^i ({}^tD_3^i)^2, \\ {}^tD_1^i &= \frac{2{}^t\sigma_1^i}{(X_i)^2} - \frac{{}^t\sigma_2^i}{(X_i)^2}, \quad {}^tD_2^i = -\frac{{}^t\sigma_1^i}{(X_i)^2} + \frac{2{}^t\sigma_2^i}{(Y_i)^2}, \quad {}^tD_3^i = \frac{2{}^t\tau_{12}^i}{(S_i)^2}. \end{aligned} \quad (\text{II.8b})$$

The initial conditions for the set of differential equations (II.8a) are given by the yield stresses at the elastoplastic transition points. Therefore, the initial conditions are expressed as

$$\begin{aligned} {}_0\sigma_1^i(\varphi_0) &= {}_0\sigma_1^i \left( \frac{1}{zA_i} \right) = -\frac{C_1^i}{A_i}, \\ {}_0\sigma_2^i(\varphi_0) &= {}_0\sigma_2^i \left( \frac{1}{zA_i} \right) = -\frac{C_2^i}{A_i}, \\ {}_0\tau_{12}^i(\varphi_0) &= {}_0\tau_{12}^i \left( \frac{1}{zA_i} \right) = \frac{C_3^i}{A_i}, \end{aligned} \quad (\text{II.8c})$$

where  $\varphi_0 = 1/(zA_i)$  is the yield deformation and

$$A_i = \sqrt{\frac{(C_1^i)^2}{(X_i)^2} - \frac{C_1^i C_2^i}{(X_i)^2} + \frac{(C_2^i)^2}{(Y_i)^2} + \frac{(C_3^i)^2}{(S_i)^2}}. \quad (\text{II.8d})$$

### EQUILIBRIUM EQUATION

The bending moment about the middle surface is expressed as

$${}^tM_i = - \int_{\sum_{j=0}^{i-1} T_j}^{\sum_{j=0}^i T_j} z^t \sigma_x^i b dz. \quad (\text{II.9})$$

The total bending moment of the section is  $2 \sum_{i=1}^k {}^tM_i$  and is equal to the external moment  ${}^tM$ , that is,

$${}^tM = 2 \sum_{i=1}^k {}^tM_i. \quad (\text{II.10})$$

The equations (II.9) and (II.10) yield

$${}^tM + 2 \sum_{i=1}^k \int_{\sum_{j=0}^{i-1} T_j}^{\sum_{j=0}^i T_j} z b [{}^t\sigma_1^i (\cos \theta_i)^2 + {}^t\sigma_2^i (\sin \theta_i)^2 - {}^t\tau_{12}^i \sin 2\theta_i] dz = 0. \quad (\text{II.11})$$

The above equation represents the equilibrium equation of the beam problem. Note that the only unknown in equation (II.11) is  ${}^t\varphi$ . Therefore,  ${}^t\varphi$  can be solved by combining equation (II.11) with equation (II.7) (in the elastic range) or equations (II.8) (in the plastic range). A load incremental procedure is employed to solve for the response  ${}^t\varphi$ .

### SECOND ORDER APPROXIMATION OF RATE CONSTITUTIVE EQUATIONS

In the plastic range, if the responses at the previous load level  $\tau$  are known, at the following load level  $t$  the constitutive equations (II.8a) can be approximated as

$$\begin{aligned} {}^t\sigma_1^i &= \tau\sigma_1^i + z \left[ -\tau A_{11}^i (\cos \theta_i)^2 - \tau A_{12}^i (\sin \theta_i)^2 + \frac{1}{2} \tau A_{13}^i \sin 2\theta_i \right] ({}^t\varphi - \tau\varphi) \\ &\quad + \frac{1}{2} z \left[ -\frac{\partial \tau A_{11}^i}{\partial \tau\varphi} (\cos \theta_i)^2 - \frac{\partial \tau A_{12}^i}{\partial \tau\varphi} (\sin \theta_i)^2 + \frac{1}{2} \frac{\partial \tau A_{13}^i}{\partial \tau\varphi} \sin 2\theta_i \right] ({}^t\varphi - \tau\varphi)^2, \\ {}^t\sigma_2^i &= \tau\sigma_2^i + z \left[ -\tau A_{12}^i (\cos \theta_i)^2 - \tau A_{22}^i (\sin \theta_i)^2 + \frac{1}{2} \tau A_{23}^i \sin 2\theta_i \right] ({}^t\varphi - \tau\varphi) \\ &\quad + \frac{1}{2} z \left[ -\frac{\partial \tau A_{12}^i}{\partial \tau\varphi} (\cos \theta_i)^2 - \frac{\partial \tau A_{22}^i}{\partial \tau\varphi} (\sin \theta_i)^2 + \frac{1}{2} \frac{\partial \tau A_{23}^i}{\partial \tau\varphi} \sin 2\theta_i \right] ({}^t\varphi - \tau\varphi)^2, \end{aligned} \quad (\text{II.12})$$

$$\begin{aligned} {}^t\tau_{12}^i &= \tau_{12}^i + z \left[ -\tau A_{13}^i (\cos \theta_i)^2 - \tau A_{23}^i (\sin \theta_i)^2 + \frac{1}{2} \tau A_{33}^i \sin 2\theta_i \right] ({}^t\varphi - \tau\varphi) \\ &+ \frac{1}{2} z \left[ -\frac{\partial \tau A_{13}^i}{\partial \tau\varphi} (\cos \theta_i)^2 - \frac{\partial \tau A_{23}^i}{\partial \tau\varphi} (\sin \theta_i)^2 + \frac{1}{2} \frac{\partial \tau A_{33}^i}{\partial \tau\varphi} \sin 2\theta_i \right] ({}^t\varphi - \tau\varphi)^2. \end{aligned}$$

Equations (II.12) are the second order approximation of the plastic constitutive equations in terms of the curvature. Note that the quantities  $\frac{\partial \tau A_{11}^i}{\partial \tau\varphi}$ ,  $\frac{\partial \tau A_{12}^i}{\partial \tau\varphi}$ ,  $\frac{\partial \tau A_{13}^i}{\partial \tau\varphi}$ ,  $\frac{\partial \tau A_{22}^i}{\partial \tau\varphi}$ ,  $\frac{\partial \tau A_{23}^i}{\partial \tau\varphi}$  and  $\frac{\partial \tau A_{33}^i}{\partial \tau\varphi}$  can be expressed in terms of the stresses and curvature at load level  $\tau$ . For instance,  $\frac{\partial \tau A_{11}^i}{\partial \tau\varphi}$  is calculated as follows: from equation (II.8b),

$$\frac{\partial \tau A_{11}^i}{\partial \tau\varphi} = -\frac{\frac{\partial \tau B_{11}^i}{\partial \tau\varphi} \tau C^i - \tau B_{11}^i \frac{\partial \tau C^i}{\partial \tau\varphi}}{(\tau C^i)^2},$$

where

$$\begin{aligned} \frac{\partial \tau B_{11}^i}{\partial \tau\varphi} &= 2(C_{11}^i)^2 \tau D_1^i \frac{\partial \tau D_1^i}{\partial \tau\varphi} + 2C_{11}^i C_{12}^i \left( \frac{\partial \tau D_1^i}{\partial \tau\varphi} \tau D_2^i + \tau D_1^i \frac{\partial \tau D_2^i}{\partial \tau\varphi} \right) + 2(C_{12}^i)^2 \tau D_2^i \frac{\partial \tau D_2^i}{\partial \tau\varphi}, \\ \frac{\partial \tau C^i}{\partial \tau\varphi} &= 2C_{11}^i \tau D_1^i \frac{\partial \tau D_1^i}{\partial \tau\varphi} + 2C_{12}^i \left( \frac{\partial \tau D_1^i}{\partial \tau\varphi} \tau D_2^i + \tau D_1^i \frac{\partial \tau D_2^i}{\partial \tau\varphi} \right) + 2C_{22}^i \tau D_2^i \frac{\partial \tau D_2^i}{\partial \tau\varphi} \\ &+ 4C_{22}^i \tau D_3^i \frac{\partial \tau D_3^i}{\partial \tau\varphi}, \\ \frac{\partial \tau D_1^i}{\partial \tau\varphi} &= \frac{2}{(X_i)^2} \frac{\partial \tau \sigma_1^i}{\partial \tau\varphi} - \frac{1}{(X_i)^2} \frac{\partial \tau \sigma_2^i}{\partial \tau\varphi}, \\ \frac{\partial \tau D_2^i}{\partial \tau\varphi} &= -\frac{2}{(X_i)^2} \frac{\partial \tau \sigma_1^i}{\partial \tau\varphi} + \frac{2}{(Y_i)^2} \frac{\partial \tau \sigma_2^i}{\partial \tau\varphi}, \\ \frac{\partial \tau D_3^i}{\partial \tau\varphi} &= \frac{2}{(S_i)^2} \frac{\partial \tau \tau_{12}^i}{\partial \tau\varphi}, \end{aligned} \quad (II.13)$$

and  $\frac{\partial \tau \sigma_1^i}{\partial \tau\varphi}$ ,  $\frac{\partial \tau \sigma_2^i}{\partial \tau\varphi}$  and  $\frac{\partial \tau \tau_{12}^i}{\partial \tau\varphi}$  are calculated using equation (II.8a). The remaining terms are to be calculated in the same fashion.

## SENSITIVITY ANALYSIS

The direct differentiation method is used for the sensitivity analysis of the beam. Once the responses at load level  $t$  have been calculated, the design sensitivities at that level can be obtained. Choosing the  $m^{\text{th}}$  ply angle  $\theta_m$  as the design variable, direct differentiation of equation (II.11) yields the sensitivity of the curvature  ${}^t\varphi$  with respect to  $\theta_m$  as

$$\frac{\partial {}^t\varphi}{\partial \theta_m} = -\frac{A + C}{B}, \quad (II.14)$$

where

$$A = \sum_{i=1}^k \int_{\sum_{j=0}^{i-1} T_j}^{\sum_{j=0}^i T_j} z (-{}^t\sigma_1^i \sin 2\theta_i + {}^t\sigma_2^i \sin 2\theta_i - 2{}^t\tau_{12}^i \cos 2\theta_i) \delta_{im} dz, \quad (II.15)$$

$$B = \sum_{i=1}^k \int_{\sum_{j=0}^{i-1} T_j}^{\sum_{j=0}^i T_j} z \left[ \frac{\partial {}^t\sigma_1^i}{\partial \theta_m} (\cos \theta_i)^2 + \frac{\partial {}^t\sigma_2^i}{\partial \theta_m} (\sin \theta_i)^2 - \frac{\partial {}^t\tau_{12}^i}{\partial \theta_m} \sin 2\theta_i \right] dz, \quad (II.16)$$

$$C = \sum_{i=1}^k \int_{\sum_{j=0}^{i-1} T_j}^{\sum_{j=0}^i T_j} z \left[ \frac{\partial {}^t\sigma_1^i}{\partial \theta_m} (\cos \theta_i)^2 + \frac{\partial {}^t\sigma_2^i}{\partial \theta_m} (\sin \theta_i)^2 - \frac{\partial {}^t\tau_{12}^i}{\partial \theta_m} \sin 2\theta_i \right] dz. \quad (II.17)$$

The quantities  ${}^t\sigma_1^i$ ,  ${}^t\sigma_2^i$  and  ${}^t\tau_{12}^i$  are calculated using equation (II.7) if the responses are elastic and equation (II.12) if the responses are plastic. The following procedure is employed to calculate the quantities  $\frac{\partial {}^t\sigma_1^i}{\partial {}^t\varphi}$ ,  $\frac{\partial {}^t\sigma_2^i}{\partial {}^t\varphi}$ , and  $\frac{\partial {}^t\tau_{12}^i}{\partial {}^t\varphi}$ . In the elastic range, direct differentiation of equation (II.7) yields

$$\begin{aligned}\frac{\partial {}^t\sigma_1^i}{\partial {}^t\varphi} &= -z [C_{11}^i (\cos \theta_i)^2 + C_{12}^i (\sin \theta_i)^2], \\ \frac{\partial {}^t\sigma_2^i}{\partial {}^t\varphi} &= -z [C_{12}^i (\cos \theta_i)^2 + C_{22}^i (\sin \theta_i)^2], \\ \frac{\partial {}^t\tau_{12}^i}{\partial {}^t\varphi} &= z C_{66}^i \sin 2\theta_i.\end{aligned}\quad (\text{II.18})$$

In the plastic range, they are calculated using equation (II.8a). As for the terms  $\frac{\partial {}^t\sigma_1^i}{\partial \theta_m}$ ,  $\frac{\partial {}^t\sigma_2^i}{\partial \theta_m}$  and  $\frac{\partial {}^t\tau_{12}^i}{\partial \theta_m}$ , in the elastic range, partial differentiation of the equation (II.7) with respect to  $\theta_m$  yields

$$\begin{aligned}\frac{\partial {}^t\sigma_1^i}{\partial \theta_m} &= -z {}^t\varphi (-C_{11}^i \sin 2\theta_i + C_{12}^i \sin 2\theta_i) \delta_{im}, \\ \frac{\partial {}^t\sigma_2^i}{\partial \theta_m} &= -z {}^t\varphi (-C_{12}^i \sin 2\theta_i + C_{22}^i \sin 2\theta_i) \delta_{im}, \\ \frac{\partial {}^t\tau_{12}^i}{\partial \theta_m} &= 2z {}^t\varphi C_{66}^i \cos 2\theta_i \delta_{im}.\end{aligned}\quad (\text{II.19})$$

In the plastic range, partial differentiation of the equation (II.8a) and the initial conditions equation (II.8c), with respect to  $\theta_m$  yields

$$\begin{aligned}\frac{\partial \left( \frac{\partial {}^t\sigma_1^i}{\partial \theta_m} \right)}{\partial {}^t\varphi} &= z \left[ -\frac{\partial {}^t A_{11}^i}{\partial {}^t\sigma_1^i} (\cos \theta_i)^2 - \frac{\partial {}^t A_{12}^i}{\partial {}^t\sigma_1^i} (\sin \theta_i)^2 + \frac{1}{2} \frac{\partial {}^t A_{13}^i}{\partial {}^t\sigma_1^i} \sin 2\theta_i \right] \frac{\partial {}^t\sigma_1^i}{\partial \theta_m} \\ &+ z \left[ -\frac{\partial {}^t A_{11}^i}{\partial {}^t\sigma_2^i} (\cos \theta_i)^2 - \frac{\partial {}^t A_{12}^i}{\partial {}^t\sigma_2^i} (\sin \theta_i)^2 + \frac{1}{2} \frac{\partial {}^t A_{13}^i}{\partial {}^t\sigma_2^i} \sin 2\theta_i \right] \frac{\partial {}^t\sigma_2^i}{\partial \theta_m} \\ &+ z \left[ -\frac{\partial {}^t A_{11}^i}{\partial {}^t\tau_{12}^i} (\cos \theta_i)^2 - \frac{\partial {}^t A_{12}^i}{\partial {}^t\tau_{12}^i} (\sin \theta_i)^2 + \frac{1}{2} \frac{\partial {}^t A_{13}^i}{\partial {}^t\tau_{12}^i} \sin 2\theta_i \right] \frac{\partial {}^t\tau_{12}^i}{\partial \theta_m} \\ &+ z ({}^t A_{11}^i \sin 2\theta_i - {}^t A_{12}^i \sin 2\theta_i + {}^t A_{13}^i \cos 2\theta_i) \delta_{im}, \\ \frac{\partial \left( \frac{\partial {}^t\sigma_2^i}{\partial \theta_m} \right)}{\partial {}^t\varphi} &= z \left[ -\frac{\partial {}^t A_{12}^i}{\partial {}^t\sigma_1^i} (\cos \theta_i)^2 - \frac{\partial {}^t A_{22}^i}{\partial {}^t\sigma_1^i} (\sin \theta_i)^2 + \frac{1}{2} \frac{\partial {}^t A_{23}^i}{\partial {}^t\sigma_1^i} \sin 2\theta_i \right] \frac{\partial {}^t\sigma_1^i}{\partial \theta_m} \\ &+ z \left[ -\frac{\partial {}^t A_{12}^i}{\partial {}^t\sigma_2^i} (\cos \theta_i)^2 - \frac{\partial {}^t A_{22}^i}{\partial {}^t\sigma_2^i} (\sin \theta_i)^2 + \frac{1}{2} \frac{\partial {}^t A_{23}^i}{\partial {}^t\sigma_2^i} \sin 2\theta_i \right] \frac{\partial {}^t\sigma_2^i}{\partial \theta_m} \\ &+ z \left[ -\frac{\partial {}^t A_{12}^i}{\partial {}^t\tau_{12}^i} (\cos \theta_i)^2 - \frac{\partial {}^t A_{22}^i}{\partial {}^t\tau_{12}^i} (\sin \theta_i)^2 + \frac{1}{2} \frac{\partial {}^t A_{23}^i}{\partial {}^t\tau_{12}^i} \sin 2\theta_i \right] \frac{\partial {}^t\tau_{12}^i}{\partial \theta_m} \\ &+ z ({}^t A_{12}^i \sin 2\theta_i - {}^t A_{22}^i \sin 2\theta_i + {}^t A_{23}^i \cos 2\theta_i) \delta_{im}, \\ \frac{\partial \left( \frac{\partial {}^t\tau_{12}^i}{\partial \theta_m} \right)}{\partial {}^t\varphi} &= z \left[ -\frac{\partial {}^t A_{13}^i}{\partial {}^t\sigma_1^i} (\cos \theta_i)^2 - \frac{\partial {}^t A_{23}^i}{\partial {}^t\sigma_1^i} (\sin \theta_i)^2 + \frac{1}{2} \frac{\partial {}^t A_{33}^i}{\partial {}^t\sigma_1^i} \sin 2\theta_i \right] \frac{\partial {}^t\sigma_1^i}{\partial \theta_m} \\ &+ z \left[ -\frac{\partial {}^t A_{13}^i}{\partial {}^t\sigma_2^i} (\cos \theta_i)^2 - \frac{\partial {}^t A_{23}^i}{\partial {}^t\sigma_2^i} (\sin \theta_i)^2 + \frac{1}{2} \frac{\partial {}^t A_{33}^i}{\partial {}^t\sigma_2^i} \sin 2\theta_i \right] \frac{\partial {}^t\sigma_2^i}{\partial \theta_m} \\ &+ z \left[ -\frac{\partial {}^t A_{13}^i}{\partial {}^t\tau_{12}^i} (\cos \theta_i)^2 - \frac{\partial {}^t A_{23}^i}{\partial {}^t\tau_{12}^i} (\sin \theta_i)^2 + \frac{1}{2} \frac{\partial {}^t A_{33}^i}{\partial {}^t\tau_{12}^i} \sin 2\theta_i \right] \frac{\partial {}^t\tau_{12}^i}{\partial \theta_m} \\ &+ z ({}^t A_{13}^i \sin 2\theta_i - {}^t A_{23}^i \sin 2\theta_i + {}^t A_{33}^i \cos 2\theta_i) \delta_{im},\end{aligned}\quad (\text{II.20a})$$

and

$$\begin{aligned}
\frac{\partial_0 \sigma_1^i}{\partial \theta_m} &= -\frac{\frac{\partial C_1^i}{\partial \theta_m} A_i - C_1^i \frac{\partial A_i}{\partial \theta_m}}{(A_i)^2} \\
&\quad + \frac{\frac{\partial A_i}{\partial \theta_m}}{(A_i)^2} \left[ -{}_0A_{11}^i (\cos \theta_i)^2 - {}_0A_{12}^i (\cos \theta_i)^2 + \frac{1}{2} {}_0A_{13}^i \sin 2\theta_i \right], \\
\frac{\partial_0 \sigma_2^i}{\partial \theta_m} &= -\frac{\frac{\partial C_2^i}{\partial \theta_m} A_i - C_2^i \frac{\partial A_i}{\partial \theta_m}}{(A_i)^2} \\
&\quad + \frac{\frac{\partial A_i}{\partial \theta_m}}{(A_i)^2} \left[ -{}_0A_{12}^i (\cos \theta_i)^2 - {}_0A_{22}^i (\cos \theta_i)^2 + \frac{1}{2} {}_0A_{23}^i \sin 2\theta_i \right], \\
\frac{\partial_0 \tau_{12}^i}{\partial \theta_m} &= -\frac{\frac{\partial C_3^i}{\partial \theta_m} A_i - C_3^i \frac{\partial A_i}{\partial \theta_m}}{(A_i)^2} \\
&\quad + \frac{\frac{\partial A_i}{\partial \theta_m}}{(A_i)^2} \left[ -{}_0A_{13}^i (\cos \theta_i)^2 - {}_0A_{23}^i (\cos \theta_i)^2 + \frac{1}{2} {}_0A_{33}^i \sin 2\theta_i \right],
\end{aligned} \tag{II.20b}$$

where the quantities  $\frac{\partial^t A_{11}^i}{\partial^t \sigma_1^i}$ ,  $\frac{\partial^t A_{12}^i}{\partial^t \sigma_1^i}$ , and  $\frac{\partial^t A_{33}^i}{\partial^t \tau_{12}^i}$  are obtained by differentiating equation (II.8b). The quantities  $\frac{\partial C_1^i}{\partial \theta_m}$ ,  $\frac{\partial C_2^i}{\partial \theta_m}$ ,  $\frac{\partial C_3^i}{\partial \theta_m}$ , and  $\frac{\partial A_i}{\partial \theta_m}$ , are obtained by differentiating equation (II.6b) and equation (II.8d), respectively, and the quantities  ${}_0A_{11}^i, \dots, {}_0A_{33}^i$  are calculated by substituting the initial yield stresses equation (II.8c) in equation (II.8b). Therefore, equations (II.20a) represent a set of linear differential equations in  $\frac{\partial^t \sigma_1^i}{\partial \theta_m}$ ,  $\frac{\partial^t \sigma_2^i}{\partial \theta_m}$ , and  $\frac{\partial^t \tau_{12}^i}{\partial \theta_m}$  with equations (II.20b) as the initial conditions. Once the set of linear differential equations is solved, the sensitivities of the curvature  $\frac{\partial^t \varphi}{\partial \theta_m}$  are calculated using equation (II.14). Then the stress sensitivities are calculated as

$$\begin{aligned}
\frac{d^t \sigma_1^i}{d\theta_m} &= \frac{\partial^t \sigma_1^i}{\partial^t \varphi} \frac{\partial^t \varphi}{\partial \theta_m} + \frac{\partial^t \sigma_1^i}{\partial \theta_m}, \\
\frac{d^t \sigma_2^i}{d\theta_m} &= \frac{\partial^t \sigma_2^i}{\partial^t \varphi} \frac{\partial^t \varphi}{\partial \theta_m} + \frac{\partial^t \sigma_2^i}{\partial \theta_m}, \\
\frac{d^t \tau_{12}^i}{d\theta_m} &= \frac{\partial^t \tau_{12}^i}{\partial^t \varphi} \frac{\partial^t \varphi}{\partial \theta_m} + \frac{\partial^t \tau_{12}^i}{\partial \theta_m}.
\end{aligned} \tag{II.21}$$

## NUMERICAL RESULTS

In the numerical calculation, the beam is assumed to be made of six layers of orthotropic Glass/Epoxy laminae with the stacking sequence  $(0^\circ/10^\circ/45^\circ)_2$ . The curvatures of the beam and the stresses of the third ply in the principal material directions and the shear stress at the top of the beam are calculated. The third ply angle is chosen to be the design variable. The sensitivities of the curvatures and the stresses with respect to the design variable are calculated. The following material properties are used:  $E_1 = 7.8 \times 10^6$  psi,  $E_2 = 2.6 \times 10^6$  psi,  $\nu_{12} = 0.25$ ,  $G_{12} = 1.3 \times 10^6$  psi,  $X = 1.5 \times 10^5$  psi,  $Y = 0.04 \times 10^5$  psi and  $S = 0.06 \times 10^5$  psi.

In the response calculation, the results of the second order approximation technique are compared with the linear approximation and the generalized Euler method. Table 1 compares the curvatures obtained using the three methods. Tables 2, 3 and 4 compare the stresses  ${}^t\sigma_1^3$ ,  ${}^t\sigma_2^3$  and  ${}^t\tau_{12}^3$ , respectively, obtained using the three methods. It can be seen that the results obtained using the second order approximation match those obtained using the generalized Euler method up to the fifth decimal point. This is because both methods have the same second order degree of accuracy [10,11]. The results obtained using the linear approximation which has first order degree of accuracy are slightly different from the results obtained using the other two methods.

The sensitivities of the curvature are calculated using the direct differentiation approach (DDA) and are compared with those obtained using central finite difference approach (CFDA). Several

Table 1. Curvature during loading.

Load $\times 10^5$ lb-in	Curvature (/in)		
	Linear	Euler	2nd-ord
0.1	0.01309	0.01309	0.01309
0.2	0.02618	0.02618	0.02618
0.3	0.03967	0.03968	0.03968
0.4	0.05647	0.05652	0.05652
0.5	0.07444	0.07453	0.07453
0.6	0.09278	0.09290	0.09290
0.7	0.11141	0.11153	0.11153
0.8	0.13026	0.13038	0.13038
0.9	0.14938	0.14951	0.14951
1.0	0.16873	0.16886	0.16886

Table 2. Stress  ${}^t\sigma_1^3$  during loading.

Load $\times 10^5$ lb-in	stress ${}^t\sigma_1^3 (\times 10^5 \text{ lb/in}^2)$		
	Linear	Euler	2nd-ord
0.1	-0.03389	-0.03389	-0.03389
0.2	-0.06778	-0.06778	-0.06778
0.3	-0.10092	-0.10092	-0.10092
0.4	-0.13908	-0.13913	-0.13913
0.5	-0.18034	-0.18044	-0.18044
0.6	-0.22252	-0.22264	-0.22264
0.7	-0.26538	-0.26550	-0.26550
0.8	-0.30874	-0.30886	-0.30886
0.9	-0.35274	-0.35285	-0.35285
1.0	-0.39721	-0.39732	-0.39732

Table 3. Stress  ${}^t\sigma_2^3$  during loading.

Load $\times 10^5$ lb-in	stress ${}^t\sigma_2^3 (\times 10^5 \text{ lb/in}^2)$		
	Linear	Euler	2nd-ord
0.1	-0.01304	-0.01304	-0.01304
0.2	-0.02607	-0.02607	-0.02607
0.3	-0.03349	-0.03349	-0.03349
0.4	-0.03124	-0.03125	-0.03125
0.5	-0.02915	-0.02917	-0.02917
0.6	-0.02748	-0.02750	-0.02750
0.7	-0.02624	-0.02626	-0.02626
0.8	-0.02535	-0.02536	-0.02536
0.9	-0.02468	-0.02469	-0.02469
1.0	-0.02419	-0.02417	-0.02417

Table 4. Stress  ${}^t\tau_{12}^3$  during loading.

Load $\times 10^5$ lb-in	stress ${}^t\tau_{12}^3 (\times 10^5 \text{ lb/in}^2)$		
	Linear	Euler	2nd-ord
0.1	0.01021	0.01021	0.01021
0.2	0.02042	0.02042	0.02042
0.3	0.02878	0.02875	0.02875
0.4	0.03388	0.03376	0.03376
0.5	0.03763	0.03746	0.03746
0.6	0.04006	0.03986	0.03986
0.7	0.04151	0.04132	0.04132
0.8	0.04230	0.04212	0.04212
0.9	0.04264	0.04248	0.04248
1.0	0.04268	0.04253	0.04253

Table 5. Sensitivity of curvature during loading.

Load $\times 10^5$ lb-in	Sensitivity of Curvature (/in)					
	CFDA			DDA		
	Linear	Euler	2nd-ord	Linear	Euler	2nd-ord
0.1	0.00922	0.00922	0.00922	0.00922	0.00922	0.00922
0.2	0.01845	0.01845	0.01845	0.01845	0.01845	0.01845
0.3	0.03458	0.03458	0.03458	0.03523	0.03523	0.03523
0.4	0.07277	0.07279	0.07279	0.07435	0.07436	0.07436
0.5	0.10070	0.10068	0.10068	0.10238	0.10238	0.10238
0.6	0.12942	0.12937	0.12938	0.13115	0.13111	0.13112
0.7	0.15851	0.15841	0.15842	0.16020	0.16012	0.16013
0.8	0.18824	0.18815	0.18816	0.18999	0.18990	0.18991
0.9	0.21942	0.21934	0.21935	0.22115	0.22105	0.22106
1.0	0.25057	0.25046	0.25047	0.25217	0.25210	0.25212

different finite difference step sizes ranging from 0.001 to 0.000001 were tried in the CFDA approach. The step size 0.00001 gave the most accurate results and was used in the paper. All three approximation techniques are used for the response analysis. Table 5 compares the results of the DDA with the results of the CFDA. The results of the generalized Euler method match those of the second order approximation up to the fourth decimal point. The results of the linear approximation match those of the second order approximation up to the third decimal point. The results of the CFDA match those of the DDA only up to the second decimal point.

Once the sensitivities of the curvatures are obtained, the constraint sensitivities are calculated using the direct differentiation of the constraint functions (or functionals). It is assumed that the constraint conditions of the third ply are described by the stresses in the principal material directions (1,2) and the shear stress in the ply plane as

$$\Pi_1 = {}^t\sigma_1^3 - X_F^3 \leq 0,$$

$$\Pi_2 = {}^t\sigma_2^3 - Y_F^3 \leq 0,$$

$$\Pi_3 = {}^t\tau_{12}^3 - S_F^3 \leq 0,$$

where  $X_F^3$ ,  $Y_F^3$  and  $S_F^3$  are the longitudinal failure strength, the transverse failure strength and the shear failure strength of the third ply, respectively, and represent the upper bounds on the stresses. Tables 6, 7 and 8 present the design sensitivities of the constraints  $\Pi_1$ ,  $\Pi_2$  and  $\Pi_3$ , respectively, with respect to the third ply angle. All three approximation techniques are used. The constraint sensitivities obtained using the DDA, show excellent agreement with each other. The second order approximation yields almost the same results as the generalized Euler approach. When these results are compared to those obtained using the CFDA, the results are in good agreement up to the elastic limit and differences are exhibited once the deformations enter the plastic range. For clarity, Figure 3 shows a comparison of the design sensitivities of constraint  $\Pi_1$ , obtained using the CFDA and the DDA when the second order approximation is used. Tables 9, 10 and 11 present the design sensitivities of the constraints  $\Pi_1$ ,  $\Pi_2$  and  $\Pi_3$ , respectively, near the yield point. For clarity, the data of Table 9 is plotted in Figure 4 and shows a comparison of the design sensitivities of constraint  $\Pi_1$  near yield points using the CFDA and the DDA with the second order approximation for stresses. It is seen that the differences increase with increase in the plastic deformations. These differences are due to the errors associated with the results obtained using the CFDA. When finite difference technique is used, in order to get a good estimate of the stress derivatives it is necessary to calculate the stresses accurately. However, in the rate constitutive problems, the stresses cannot be calculated directly. Only their approximate values are obtained using numerical approaches (e.g., the linear approximation, the generalized Euler method or the higher order approximation). As the plastic deformations increase, the approximations fail to provide accurate results due to the nonlinearity of the problem. Therefore, the stress sensitivities, calculated from these stress values, are unreliable in this range.

Table 6. Sensitivity of constraint  $\Pi_1$  during loading.

Load $\times 10^5$ lb-in	Sensitivity of constraint $\Pi_1 (\times 10^5 \text{ lb/in}^2)$					
	CFDA			DDA		
	Linear	Euler	2nd-ord	Linear	Euler	2nd-ord
0.1	0.02790	0.02790	0.02790	0.02790	0.02790	0.02790
0.2	0.05580	0.05580	0.05580	0.05580	0.05580	0.05580
0.3	0.07028	0.07028	0.07028	0.07526	0.07526	0.07526
0.4	0.05760	0.05760	0.05760	0.07673	0.07683	0.07682
0.5	0.07326	0.07326	0.07327	0.09232	0.09252	0.09251
0.6	0.08875	0.08875	0.08875	0.10756	0.10793	0.10793
0.7	0.10456	0.10456	0.10456	0.12333	0.12369	0.12369
0.8	0.11978	0.11078	0.11978	0.13847	0.13886	0.13886
0.9	0.13322	0.13322	0.13322	0.15331	0.15261	0.15261
1.0	0.14765	0.14756	0.14764	0.16703	0.16743	0.16743

When the material enters the plastic range, the unloading is history-dependent. In the example considered, the load at the initial instant of unloading is  $0.4 \times 10^5$  lb-in. The unloading process conforms the generalized Hooke's law. Table 12 presents the curvature values during unloading. Tables 13, 14 and 15 present the stresses during unloading. The second order approximation and

Table 7. Sensitivity of constraint  $\Pi_2$  during loading.

Load $\times 10^5$ lb-in	Sensitivity of constraint $\Pi_2 (\times 10^5 \text{ lb/in}^2)$					
	CFDA			DDA		
	Linear	Euler	2nd-ord	Linear	Euler	2nd-ord
0.1	-0.02069	-0.02069	-0.02069	-0.02069	-0.02069	-0.02069
0.2	-0.04138	-0.04138	-0.04138	-0.04138	-0.04138	-0.04138
0.3	-0.06491	-0.06491	-0.06491	-0.04497	-0.04498	-0.04498
0.4	-0.07300	-0.07300	-0.07300	0.00180	0.00182	0.00182
0.5	-0.07206	-0.07206	-0.07206	0.00117	0.00121	0.00121
0.6	-0.07123	-0.07123	-0.07123	-0.00073	-0.00062	-0.00063
0.7	-0.07055	-0.07055	-0.07055	-0.00340	-0.00324	-0.00324
0.8	-0.07000	-0.07000	-0.07000	-0.00628	-0.00607	-0.00607
0.9	-0.06956	-0.06955	-0.06955	-0.00898	-0.00875	-0.00875
1.0	-0.06930	-0.06930	-0.06929	-0.01134	-0.01112	-0.01113

Table 8. Sensitivity of constraint  $\Pi_3$  during loading.

Load $\times 10^5$ lb-in	Sensitivity of constraint $\Pi_3 (\times 10^5 \text{ lb/in}^2)$					
	CFDA			DDA		
	Linear	Euler	2nd-ord	Linear	Euler	2nd-ord
0.1	0.00599	0.00599	0.00599	0.00599	0.00599	0.00599
0.2	0.01199	0.01199	0.01199	0.01199	0.01199	0.01199
0.3	0.02179	0.02177	0.02177	0.01460	0.01460	0.01460
0.4	0.03648	0.03629	0.03629	0.00451	0.00457	0.00457
0.5	0.04350	0.04326	0.04326	0.00276	0.00293	0.00293
0.6	0.04913	0.04888	0.04888	-0.00056	-0.00027	-0.00027
0.7	0.05362	0.05337	0.05337	-0.00436	-0.00399	-0.00399
0.8	0.05726	0.05703	0.05703	-0.00792	-0.00749	-0.00749
0.9	0.06028	0.06007	0.06007	-0.01091	-0.01045	-0.01046
1.0	0.06278	0.06260	0.06260	-0.01328	-0.01282	-0.01282

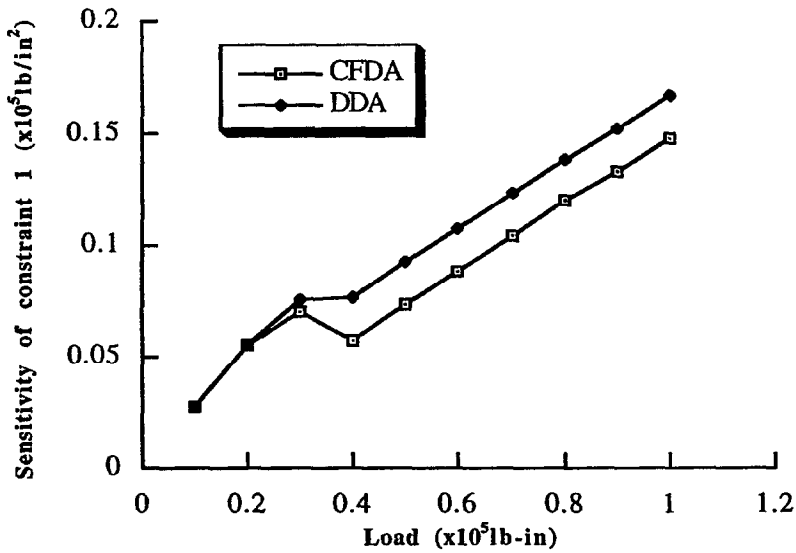


Figure 3. Comparison of sensitivities of constraint ( $\Pi_1$ ); direct difference approach (DDA) and central finite difference approach (CFDA).

the generalized Euler method produce the same results. The linear approximation also shows very good agreement with the other two techniques. Table 16 presents the sensitivities of the

Table 9. Sensitivity of constraint  $\Pi_1$  near yield point during loading.

Load $\times 10^5$ lb-in	Sensitivity of constraint $\Pi_1 (\times 10^5 \text{ lb/in}^2)$					
	CFDA			DDA		
	Linear	Euler	2nd-ord	Linear	Euler	2nd-ord
0.26875	0.07498	0.07498	0.07498	0.07498	0.07498	0.07498
0.27500	0.07515	0.07515	0.07515	0.07588	0.07588	0.07588
0.28125	0.07390	0.07390	0.07390	0.07566	0.07566	0.07566
0.28750	0.07267	0.07267	0.07267	0.07564	0.07564	0.07564
0.29375	0.07142	0.07142	0.07142	0.07542	0.07542	0.07542
0.30000	0.07017	0.07017	0.07017	0.07531	0.07531	0.07531

Table 10. Sensitivity of constraint  $\Pi_2$  near yield point during loading.

Load $\times 10^5$ lb-in	Sensitivity of constraint $\Pi_2 (\times 10^5 \text{ lb/in}^2)$					
	CFDA			DDA		
	Linear	Euler	2nd-ord	Linear	Euler	2nd-ord
0.26875	-0.05560	-0.05560	-0.05560	-0.05560	-0.05560	-0.05560
0.27500	-0.05743	-0.05743	-0.05743	-0.05509	-0.05509	-0.05509
0.28125	-0.05962	-0.05962	-0.05962	-0.05271	-0.05271	-0.05271
0.28750	-0.06167	-0.06167	-0.06167	-0.05049	-0.05049	-0.05049
0.29375	-0.06358	-0.06358	-0.06358	-0.04758	-0.04758	-0.04758
0.30000	-0.06534	-0.06534	-0.06534	-0.04490	-0.04490	-0.04490

Table 11. Sensitivity of constraint  $\Pi_3$  near yield point during loading.

Load $\times 10^5$ lb-in	Sensitivity of constraint $\Pi_3 (\times 10^5 \text{ lb/in}^2)$					
	CFDA			DDA		
	Linear	Euler	2nd-ord	Linear	Euler	2nd-ord
0.26875	0.01611	0.01611	0.01611	0.01611	0.01611	0.01611
0.27500	0.01695	0.01695	0.01695	0.01611	0.01611	0.01611
0.28125	0.01821	0.01820	0.01820	0.01579	0.01579	0.01579
0.28750	0.01944	0.01944	0.01944	0.01548	0.01548	0.01548
0.29375	0.02067	0.02066	0.02066	0.01501	0.01502	0.01502
0.30000	0.02188	0.02187	0.02187	0.01459	0.01460	0.01460

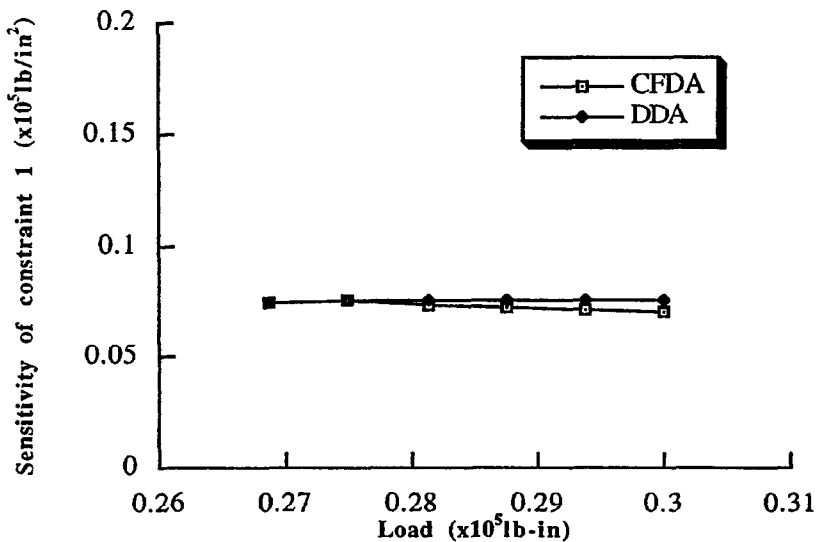


Figure 4. Comparison of sensitivities of constraint ( $\Pi_1$ ) near yield point; direct difference approach (DDA) and central finite difference approach (CFDA).

Table 12. Curvature during unloading.

Load × 10 <sup>5</sup> lb-in	Curvature (/in)		
	Linear	Euler	2nd-ord
0.4	0.05647	0.05652	0.05652
0.35	0.04961	0.04963	0.04963
0.3	0.04307	0.04309	0.04309
0.25	0.03652	0.03654	0.03654
0.2	0.02998	0.03000	0.03000
0.15	0.02343	0.02345	0.02345
0.1	0.01689	0.01691	0.01691
0.05	0.01034	0.01036	0.01036
0.0	0.00380	0.00382	0.00382

Table 13. Stress  ${}^t\sigma_1^3$  during unloading.

Load × 10 <sup>5</sup> lb-in	stress ${}^t\sigma_1^3$ (× 10 <sup>5</sup> lb/in <sup>2</sup> )		
	Linear	Euler	2nd-ord
0.4	-0.13908	-0.13913	-0.13913
0.35	-0.12213	-0.12218	-0.12218
0.3	-0.10519	-0.10524	-0.10524
0.25	-0.08824	-0.08829	-0.08829
0.2	-0.07130	-0.07135	-0.07135
0.15	-0.05435	-0.05440	-0.05440
0.1	-0.03740	-0.03745	-0.03745
0.05	-0.02046	-0.02051	-0.02051
0.0	-0.00351	-0.00356	-0.00356

Table 14. Stress  ${}^t\sigma_2^3$  during unloading.

Load × 10 <sup>5</sup> lb-in	stress ${}^t\sigma_2^3$ (× 10 <sup>5</sup> lb/in <sup>2</sup> )		
	Linear	Euler	2nd-ord
0.4	-0.03124	-0.03125	-0.03125
0.35	-0.02472	-0.02473	-0.02473
0.3	-0.01820	-0.01821	-0.01821
0.25	-0.01169	-0.01170	-0.01170
0.2	-0.00517	-0.00518	-0.00518
0.15	0.00135	0.00134	0.00134
0.1	0.00787	0.00786	0.00786
0.05	0.01438	0.01437	0.01437
0.0	0.02090	0.02089	0.02089

Table 15. Stress  ${}^t\tau_{12}^3$  during unloading.

Load × 10 <sup>5</sup> lb-in	stress ${}^t\tau_{12}^3$ (× 10 <sup>5</sup> lb/in <sup>2</sup> )		
	Linear	Euler	2nd-ord
0.4	0.03388	0.03376	0.03376
0.35	0.02877	0.02865	0.02865
0.3	0.02367	0.02355	0.02355
0.25	0.01856	0.01844	0.01844
0.2	0.01346	0.01334	0.01334
0.15	0.00835	0.00823	0.00823
0.1	0.00325	0.00313	0.00313
0.05	-0.00186	-0.00198	-0.00198
0.0	-0.00696	-0.00708	-0.00708

Table 16. Sensitivities of curvature during unloading.

Load × 10 <sup>5</sup> lb-in	Sensitivity of Curvature (/in)					
	CFDA			DDA		
	Linear	Euler	2nd-ord	Linear	Euler	2nd-ord
0.4	0.07429	0.07435	0.07435	0.07430	0.07436	0.07436
0.35	0.06877	0.06882	0.06883	0.06878	0.06884	0.06885
0.3	0.06416	0.06423	0.06423	0.06417	0.06424	0.06424
0.25	0.05954	0.05962	0.05963	0.05954	0.05963	0.05963
0.2	0.05491	0.05499	0.05598	0.05492	0.05498	0.05498
0.15	0.05032	0.05038	0.05039	0.05033	0.05039	0.05040
0.1	0.04251	0.04257	0.04258	0.04252	0.04258	0.04259
0.05	0.03353	0.03358	0.03359	0.03354	0.03359	0.03360
0.0	0.02541	0.02546	0.02547	0.02541	0.02547	0.02547

curvatures during unloading. Tables 17, 18 and 19 present the sensitivities of the stresses during unloading. The second approximation and the generalized Euler method give the same results. The results obtained using the linear approximation also give very good agreement with the others.

The DDA approach developed saves significant computational effort in the sensitivity analysis. Figure 5 presents a comparison of the CPU time utilized in calculating the sensitivities of constraint ( $\Pi_1$ ), using the three different approaches for response calculations, and shows 40 percent CPU saving.

Table 17. Sensitivities of stress  ${}^t\sigma_1^3$  during unloading.

Load $\times 10^5$ lb-in	Sensitivity of stress ${}^t\sigma_1^3 (\times 10^5 \text{ lb/in}^2)$					
	CFDA			DDA		
	Linear	Euler	2nd-ord	Linear	Euler	2nd-ord
0.4	0.07672	0.07683	0.07682	0.07673	0.07683	0.07683
0.35	0.06278	0.06287	0.06288	0.06278	0.06288	0.06289
0.3	0.04882	0.04893	0.04892	0.04883	0.04893	0.04892
0.25	0.03487	0.03498	0.03497	0.03488	0.03498	0.03497
0.2	0.02093	0.02102	0.02102	0.02093	0.02103	0.02103
0.15	0.00699	0.00708	0.00707	0.00698	0.00708	0.00708
0.1	-0.00001	0.00000	0.00000	-0.00001	0.00000	0.00000
0.05	-0.00457	-0.00447	-0.00448	-0.00456	-0.00447	-0.00448
0.0	-0.01094	-0.01086	-0.01086	-0.01095	-0.01085	-0.01085

Table 18. Sensitivities of stress  ${}^t\sigma_2^3$  during unloading.

Load $\times 10^5$ lb-in	Sensitivity of stress ${}^t\sigma_2^3 (\times 10^5 \text{ lb/in}^2)$					
	CFDA			DDA		
	Linear	Euler	2nd-ord	Linear	Euler	2nd-ord
0.4	0.01800	0.01819	0.01918	0.01800	0.01820	0.01820
0.35	0.01205	0.01216	0.01215	0.01206	0.01215	0.01215
0.3	0.02238	0.02250	0.02251	0.02239	0.02251	0.02251
0.25	0.03271	0.03285	0.03285	0.03284	0.03286	0.03286
0.2	0.04307	0.04319	0.04320	0.04309	0.04321	0.04320
0.15	0.05340	0.05353	0.05352	0.05339	0.05352	0.05352
0.1	0.06639	0.06653	0.06654	0.06638	0.06653	0.06653
0.05	0.08037	0.08051	0.08052	0.08036	0.08052	0.08052
0.0	0.09364	0.09376	0.09376	0.09366	0.09377	0.09377

Table 19. Sensitivities of stress  ${}^t\tau_{12}^3$  during unloading.

Load $\times 10^5$ lb-in	Sensitivity of stress ${}^t\tau_{12}^3 (\times 10^5 \text{ lb/in}^2)$					
	CFDA			DDA		
	Linear	Euler	2nd-ord	Linear	Euler	2nd-ord
0.4	0.00451	0.00457	0.00456	0.00451	0.00457	0.00457
0.35	0.00151	0.00158	0.00158	0.00152	0.00157	0.00157
0.3	-0.00148	-0.00142	-0.00142	-0.00148	-0.00142	-0.00142
0.25	-0.00447	-0.00441	-0.00441	-0.00448	-0.00442	-0.00442
0.2	-0.00748	-0.00741	-0.00742	-0.00748	-0.00742	-0.00742
0.15	-0.01048	-0.01042	-0.01043	-0.01047	-0.01042	-0.01042
0.1	-0.01555	-0.01551	-0.01550	-0.01556	-0.01550	-0.01550
0.05	-0.02141	-0.02133	-0.02134	-0.02140	-0.02134	-0.02134
0.0	-0.02669	-0.02661	-0.02662	-0.02668	-0.02661	-0.02662

## CONCLUDING REMARKS

A nonlinear sensitivity analysis procedure was developed for the analysis of elastoplastic structures. The formulation involved composite materials with material nonlinearity. The sensitivity analysis was based on a direct differentiation approach and the responses were calculated using a load incrementation technique. In the response analysis, a higher order approximation of the integration of the rate constitutive equation was used. The design sensitivity equation was obtained by direct differentiation of the equilibrium equation with respect to the design variables. In the

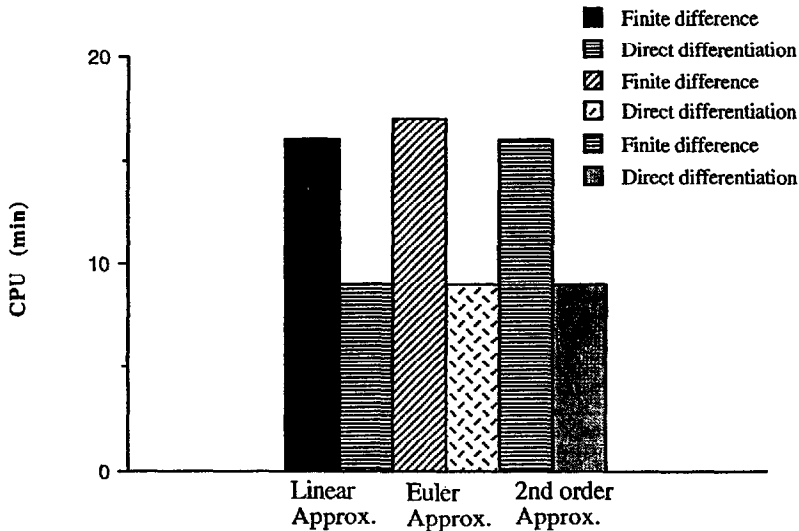


Figure 5. Comparison of CPU time in constraint ( $\Pi_1$ ) sensitivity calculation.

sensitivity analysis, a partial differentiation of the rate constitutive equations with respect to the design variable was proposed. Using this approach, the discontinuities of the design sensitivities at the material transition points were prevented from affecting the design sensitivities at other points. The following important observations were made.

(1) *Approximation of the rate constitutive equations.* This approximation is reinforced in the response analysis and shows excellent agreement with the generalized Euler approach.

(2) *Design partial differentiation of the rate constitutive equations.* This procedure is used in the sensitivity analysis to obtain the partial derivatives of the stresses with respect to the design variables and yields a set of linear differential equations which are relatively easy to solve. This avoids expensive time integration which is commonly used. The procedure requires partial derivatives of yield stresses with respect to design variables, displacements and stresses after the yield point, but does not require the previous sensitivity information. This avoids the problem of discontinuities in design sensitivities at material transition point.

(3) In calculations of curvature sensitivities, the results of the direct differentiation approach show excellent agreement with those obtained using the central finite difference technique.

(4) In calculations of stress sensitivities, the results of the direct differentiation approach deviate from those obtained using the finite difference approach in the plastic range. This is due to the errors associated with the approximate calculation of the stresses in the finite difference approach.

## REFERENCES

1. J.J. Tsay and J.S. Arora, Nonlinear structural design sensitivity analysis for path dependent problems. Part 1: General Theory, *Computer Methods in Applied Mechanics and Engineering* **81**, 183–208 (1990).
2. J.J. Tsay, J.E.B. Cardoso and J.S. Arora, Nonlinear structural design sensitivity analysis for path dependent problems. Part 2: Analytical examples, *Computer Methods in Applied Mechanics and Engineering* **81**, 209–228 (1990).
3. C.A. Vidal, H.S. Lee and R.B. Haber, The consistent tangent operator for design sensitivity analysis of history-dependent response, *Comp. Systems in Engrg.* **2**, 509–523 (1991).
4. T.H. Lee and J.S. Arora, Numerical implementation of design sensitivity analysis of elastoplastic structures, *The 34<sup>th</sup> AIAA/ASME/ASCE/AHS/ASC Structures, Structural Dynamics and Materials Conference AIAA/ASME Adaptive Structures Forum*, La Jolla, CA, April 19–22, pp. 1941–1951 (1993).
5. K.J. Bathe, *Finite Element Procedures in Engineering Analysis*, Prentice-Hall, Englewood Cliffs, NJ, (1982).
6. J. Lubliner, *Plasticity Theory*, Macmillan, New York, (1990).
7. K. Chandrashekhara, General nonlinear bending analysis of composite beams, plates and shells, *Proceedings of International Conference on Composite Materials and Structures*, January 6–9, Madras, India, 392–402 (1988).
8. L.M. Kachanov, *Foundations of the Theory of Plasticity*, North-Holland, Amsterdam, (1971).

9. R.M. Jones, *Mechanics of Composite Materials*, Hemisphere, (1975).
10. K.E. Atkinson, *An Introduction to Numerical Analysis*, John Wiley & Sons, Inc., (1989).
11. W.A. Smith, *Elementary Numerical Analysis*, Harper & Row, (1979).